RESEARCH REPORT

VTT-R-03253-13

Structural Applications of Ferritic Stainless Steels (SAFSS)
WP2: Structural performance of steel members

Recommendations for the use of Direct Strength Method

Authors: Petr Hradil, Asko Talja

Confidentiality: Confidential until May 2014

Report's title	
SAFSS WP2: Recommendations for the use of DSM	
Customer, contact person, address Commission of the European Communities	**Order reference** RFSR-CT-2010-00026
Project name Structural Applications of Ferritic Stainless Steels	**Project number/Short name** 39594/SAFSS
Author(s) Petr Hradil, Asko Talja	**Pages** 57 p.
Keywords stainless steel, direct strength method, buckling	**Report identification code** VTT-R-03253-13

Summary

This report seeks to develop the necessary information which will enable comprehensive guidance on the use of Direct Strength Method for the design of ferritic stainless steel members. Direct Strength Method (DSM) is a modern simulation-based method developed specially for the design of thin-walled steel members, not yet included in the Eurocodes, but implemented in US and Australian design codes. The study addresses key factors which are required in order to demonstrate the performance of ferritic stainless steels e.g. in lattice roof trussed and space frame structures. The study is mainly based on modern numerical methods (particularly geometrically and materially non-linear analysis of the imperfect structure) to verify current closed-form or semi-numerical approaches. The necessary steps to develop design recommendations using the DSM are proposed. DSM may be an alternative approach included in an appendix to EN 1993-1-4 in the future.

Confidentiality	Confidential until May 2014

Espoo 13.5.2013

Written by	Reviewed by	Accepted by
Petr Hradil Research Scientist	Asko Talja Senior Research Scientist	Eila Lehmus Technology Manager

VTT's contact address
P.O. Box 1000, FI-02044 VTT, Finland

Distribution (customer and VTT)

Project group	1 pdf copy in project workspace
VTT/Register Office	1 copy

Preface

Direct Strength Method (DSM) is a modern simulation-based method developed specially for the design of thin-walled steel members, not yet included in the Eurocodes, but implemented in US and Australian design codes. The method is predicated upon the idea that if an engineer determines all of the elastic instabilities for the member and its gross section (i.e. local, distortional, and global buckling) and the load (or moment) that causes the section to yield, then the strength can be directly determined. A geometrically and materially non-linear with imperfections analysis (GMNIA) is used to provide data for comparison with the current methods and DSM calculations.

Espoo 13.5.2013

Authors

Contents

Abbreviations

AISI	American Iron and Steel Institute
ASCE	American Society of Civil Engineers
AS/NZS	Australian Standard/New Zealand Standard
CEN	European Committee for Standardization
CSM	Continuous Strength Method
DSM	Direct Strength Method
EN	European Standards
FB	Flexural buckling
FEM	Finite Element Method
FSM	Finite Strip Method
GBT	Generalized Beam Theory
GMNIA	Geometrically + materially nonlinear analysis with imperfections
LEA	Linear Eigenvalue Analysis
LTB	Lateral-torsional buckling
TB, TFB	Torsional buckling, Torsional-flexural buckling

Related standards

AISI S100-2007	North American Specification for the Design of Cold-Formed Steel Structural Members (AISI, 2007)
AISI S100-2007-C	Commentary on North American Specification for the Design of Cold-Formed Steel Structural Members (AISI, 2007)
AS/NZS 4600:2005	Australian/New Zealand Standard™ Cold-formed steel structures (AS/NZS, 2005)
AS/NZS 4673:2001	Australian/New Zealand Standard™ Cold-formed stainless steel structures (AS/NZS, 2001)
EN 1993-1-1	Eurocode 3: Design of steel structures – Part 1-1: General rules and rules for buildings (CEN, 2006)
EN 1993-1-3	Eurocode 3: Design of steel structures – Part 1-3: General rules - Supplementary rules for cold-formed members and sheeting (CEN, 2006)
EN 1993-1-4	Eurocode 3: Design of steel structures – Part 1-4: General rules - Supplementary rules for stainless steels (CEN, 2006)
EN 1993-1-5	Eurocode 3: Design of steel structures – Part 1-5: Plated structural elements (CEN, 2006)
SEI/ASCE 8-02	Specification for the Design of Cold-Formed Stainless Steel Structural Members (SEI/ASCE 2002)

1 Introduction

The Direct Strength Method (DSM), an alternative calculation of cold-formed steel resistance of members, taking into account the interactions of local, distortional and overall buckling. It has been introduced in American and Australian/New Zealand standards AISI S100 and AS/NZS 4600 based on [1–4].

The detailed overview of design methods used in current standards that are proposed for the use in evaluation of cross-section and member resistance is presented in the "Review of available data" report [5]. The background for the local buckling calculation is included in Appendix C of this report. This section will mostly focus on the description of DSM and methods connected to DSM.

The calculation methods presented below are deliberately written in the form of design rules in EN 1993. Therefore the nominal buckling resistance N_b is used instead of axial strength P_n from ASCE 8-02 and AISI S100 specification or nominal member capacity N_c from AS/NZS 4600 and 4673. The critical buckling length L_{cr} equals to the KL term in AISI/ASCE specification and kl term in AS/NZS. The nondimensional slenderness λ and the radius of gyration r from AISI/ASCE specification and AS/NZS are written as $\bar{\lambda}$ and i respectively according to the form used in EN.

2 Member resistance

The nominal member resistances of columns and beams in Eq. (1) are reduced cross-sectional resistances Af_y and Wf_y respectively.

$$N_b = \chi A f_y \text{ for columns}$$
$$M_b = \chi W f_y \text{ for beams.} \tag{1}$$

The reduction factors χ are not used in ASCE and AS/NZS standards, where the reduced member strength is calculated directly.

2.1 Ayrton-Perry formula

The buckling strength reduction χ can be calculated by the formula proposed by Ayrton and Perry [6] that is represented in Eqs. (2) and (3) in a form used in EN 1993 where N_{cr} and M_{cr} are the elastic buckling loads.

$$\chi = \frac{1}{\varphi + \sqrt{\varphi^2 - \bar{\lambda}^2}} \quad (\leq 1) \tag{2}$$

$$\bar{\lambda} = \sqrt{\frac{Af_y}{N_{cr}}} \text{ for columns and } \bar{\lambda} = \sqrt{\frac{Wf_y}{M_{cr}}} \text{ for beams.} \tag{3}$$

The calculation of coefficient ϕ recommended by EN 1993 is based on two parameters α and $\bar{\lambda}_0$ (Eq. (4)) that are calibrated by the experiments for different buckling modes and cross-sections.

$$\varphi = 0,5\left[1+\alpha\left(\bar{\lambda}-\bar{\lambda}_0\right)+\bar{\lambda}^2\right] \tag{4}$$

Four parameters α, β, $\bar{\lambda}_0$ and $\bar{\lambda}_1$ are required by the alternative method of AS/NZS 4673 (see Eq. (5)), and therefore the buckling curve can describe more accurately materials with rounded stress-strain relationship.

$$\varphi = 0,5\left(1+\eta+\bar{\lambda}^2\right) \text{ and } \eta = \alpha\left[\left(\bar{\lambda}-\bar{\lambda}_1\right)^{\beta}-\bar{\lambda}_0\right]. \tag{5}$$

2.2 Tangent modulus approach

The tangent method in ASCE 8-02 specification and AS/NZS 4673 is based on the iterative calculation of critical buckling strength of materials with Ramberg-Osgood constitutive model [7]. Here it is represented in the form compatible with EN 1993 in Eqs. (6) and (7) where n stands for the nonlinear factor from the Rambeg-Osgood model.

$$\chi = \frac{1}{\bar{\lambda}^2} \quad (\leq 1). \tag{6}$$

$$\begin{aligned} \bar{\lambda} &= \sqrt{\frac{Af_y}{N_{cr}}}\sqrt{1+0.002n\frac{E}{f_y}\chi^{n-1}} \text{ for columns} \\ \bar{\lambda} &= \sqrt{\frac{Wf_y}{M_{cr}}}\sqrt{1+0.002n\frac{E}{f_y}\chi^{n-1}} \text{ for beams.} \end{aligned} \tag{7}$$

2.3 Combined Ayrton-Perry formula and tangent modulus approach

The use of nondimensional slenderness calculated by the tangent method in Eq. (7) in Ayrton-Perry formula (Eq. (2)) was proposed by Hradil et al. [8]. It accounts for the initial imperfections and gradual yielding at the same time. The method requires iterative calculations in the same way as the original tangent method.

2.4 North American specification AISI S100-2007

The AISI S100 specification for the design of cold-formed steel structural members provides rules generally applicable to carbon steels. The method is, however, noted herewith because the AISI specification includes also DSM curves for the interaction of local and overall buckling that are compatible with the Eq. (8).

$$\chi = \begin{cases} 0,658^{\bar{\lambda}^2} & for\ \bar{\lambda} \leq 1,5 \\ \dfrac{0,877}{\bar{\lambda}^2} & for\ \bar{\lambda} > 1,5 \end{cases} \text{ for columns} \tag{8}$$

$$\chi = \begin{cases} 1 & for\ \overline{\lambda} \le 0,6 \\ 1,11 - 0,309\overline{\lambda} & for\ 1,6 > \overline{\lambda} \le 1,34 \\ \dfrac{1}{\overline{\lambda}^2} & for\ \overline{\lambda} > 1,34 \end{cases} \text{ for beams.}$$

3 Cross-section resistance

3.1 Effective cross-section

The method for evaluation of local buckling used in current EN 1993 is based on reduction of the cross-sectional area of Class 4 cross-sections by omitting parts of the section that are subjected to local buckling and which are thus ineffective in overall member resistance. The effect of distortional buckling of stiffeners is accounted for by reducing the thickness of outstanding parts of the effective section. The resulting cross-section may have shift in centroid position leading to the combination of compression and bending. Iterative calculations are needed for the effective width of plates subjected to bending due to the shift of section centroid and also due to the reduced thickness of outstanding stiffeners of open sections.

$$N_b = \chi A_{eff} f_y \text{ for columns}$$
$$M_b = \chi W_{eff} f_y \text{ for beams.} \qquad (9)$$

This effective cross-section approach is employed in EN 1993, AISI S100, ASCE 8-02, AS/NZS 4600 and 4673. However, there are fundamental differences in the standards:

(a) The effective section is independent on the overall buckling resistance and the plate slenderness is based on the yield strength f_y and the critical stress σ_{cr} as in Eq. (10). Then the reduction factor χ for member buckling is calculated from these effective section properties. This method is used in EN 1993.

$$\overline{\lambda}_p = \sqrt{\frac{f_y}{\sigma_{cr}}}. \qquad (10)$$

(b) The member buckling resistance for overall buckling is calculated using the full cross-section. Then the effective section is calculated using the member buckling stress χf_y (Eq. (11)). This method is employed in AISI/ASCE and AS/NZS standards. It was also recommended for the Eurocode by Talja and Salmi [9] already in 1994.

$$\overline{\lambda}_p = \sqrt{\frac{\chi f_y}{\sigma_{cr}}}. \qquad (11)$$

3.2 Direct strength method

The basics of the Direct Strength Method (DSM) are described in [5]. This method was recently included in the North American and Australian standards for carbon steel cold formed members AISI S100 and AS/NZS 4600. Its modification for stainless steels was proposed by Becque et al. [10] in combination with all major stainless steel design standards including the Eurocode. In this method, the reduced member strength f is calculated directly from the strength curves. These curves are defined in AISI S100 and AS/NZS 4600 standards in a form similar to Equation (12).

$$f = \begin{cases} f_y & \text{for } \lambda \le \lambda_{\lim} \\ \left[K_1 - K_2\left(\frac{\sigma_{cr}}{f_y}\right)^{K3}\right]\left(\frac{\sigma_{cr}}{f_y}\right)^{K4} f_y & \text{for } \lambda > \lambda_{\lim} \end{cases}, \text{ where } \lambda = \sqrt{\frac{f_y}{\sigma_{cr}}}. \tag{12}$$

The Equation (12) can be written also as Equation (13) provided that $C_1 = K_1$, $C_2 = K_2$, $C_3 = 2K_4$ and $C_4 = 2(K_3 + K_4)$. We will use Eq. (13) in this report, which is more consistent with the original theories.

$$f = \begin{cases} f_y & \text{for } \lambda \le \lambda_{\lim} \\ \left(\frac{C_1}{\lambda^{C3}} - \frac{C_2}{\lambda^{C4}}\right) f_y & \text{for } \lambda > \lambda_{\lim} \end{cases}, \text{ where } \lambda = \sqrt{\frac{f_y}{\sigma_{cr}}}. \tag{13}$$

Currently, the method covers distortional buckling and local-overall buckling interaction in compression or bending. The interaction of local and distortional buckling and distortional and overall buckling is considered insignificant, and therefore is not included in the current DSM formulation [2]. The rules for shear buckling and combined shear and bending were recently proposed by Pham and Hancock [11].

The Direct Strength Method use is limited to pre-qualified column and beam cross-sections. They include lipped C-sections, lipped C-sections with web stiffener(s), Z-sections, hats, racks upright (only compression) and trapezoids (only bending). The geometric and material limits of those sections recommended by AISI S100 and AS/NZS 4600 are presented in Appendix A. Cold-formed sections that do not satisfy the limits can still be used with additional penalization presented in the codes.

(a) Local and overall buckling interaction

The interaction of local (plate) buckling and overall (member) buckling can be calculated by DSM as the reduction of member strength in Eq. (14). The reduction factor of member buckling χ is discussed in previous chapters.

$$N_b = \chi A f_l \text{ for columns}$$

$$M_b = \chi W f_l \text{ for beams.} \tag{14}$$

The calculation in Eq. (15) is based on the knowledge of the overall buckling reduction factor χ and the critical local buckling stress $\sigma_{cr,l}$ that can be obtained for instance by the Finite Strip Method (FSM) or manually by Eq. (16), as recommended by AISI S100. The manual method is, however, providing poor prediction since it does not account for the interaction between elements.

$$f_l = \begin{cases} f_y & \text{for } \lambda_l \le \lambda_{l,\lim} \\ \left(\frac{C_1}{\lambda_l^{C3}} - \frac{C_2}{\lambda_l^{C4}} \right) f_y & \text{for } \lambda_l > \lambda_{l,\lim} \end{cases}, \text{ where } \lambda_l = \sqrt{\frac{\chi f_y}{\sigma_{cr,l}}}. \quad (15)$$

$$\sigma_{cr,l} = k \frac{\pi^2 E}{12\left(1-\nu^2\right)} \left(\frac{t}{b}\right)^2 \text{ for each plate element.} \quad (16)$$

The parameters C_1 to C_4 and $\lambda_{b,l,lim}$, recommended by Becque et al. [10] and Bezkorovainy et al. [12], are presented in Table 1 to be used with different standardized overall buckling calculation methods. It should be noted that parameters by Bezkorovainy et al. [12] were obtained from the plate buckling analysis and have a poor match to the real cross-sectional behaviour because they do not account for the corner areas of cold-formed profiles.

Table 1. DSM parameters for interaction of overall and local buckling of members.

	C_1	C_2	C_3	C_4	$\lambda_{l,lim}$
Johnson and Winter [13]	1.00	0.22	1.0	2.0	0.673
Bezkorovainy et al. [12]	0.90	0.20	1.0	2.0	0.500
Becque et al. (EN 1993-1-4) [10]	0.95	0.22	1.0	2.0	0.550
Becque et al. (AS/NZS 4673) [10]	0.95	0.22	0.8	1.6	0.474
Becque et al. (ASCE 8-02) [10]	0.90	0.20	0.9	1.8	0.463
AISI S100, AS/NZS 4600 [14, 15]	1.00	0.15	0.8	1.6	0.776

(b) Distortional buckling

In AISI S100 and AS/NZS 4600, DSM also offers a method for calculation of distortional buckling resistance. It can be written as a reduction of member strength – so the Eq. (17) will be similar to the basic formula from EN 1993.

$$N_b = Af_d \text{ for columns}$$

$$M_b = Wf_d \text{ for beams.} \quad (17)$$

The calculation of reduced strength in Eq. (18) is based on the knowledge of the critical distortional buckling stress $\sigma_{cr,d}$ that can be obtained for instance by the Finite Strip Method (FSM).

$$f_d = \begin{cases} f_y & \text{for } \lambda_d \le \lambda_{d,\lim} \\ \left(\frac{C_1}{\lambda_l^{C3}} - \frac{C_2}{\lambda_l^{C4}} \right) f_y & \text{for } \lambda_d > \lambda_{d,\lim} \end{cases}, \text{ where } \lambda_d = \sqrt{\frac{f_y}{\sigma_{cr,d}}}. \quad (18)$$

The parameters C_1 to C_4 and $\lambda_{d,lim}$ recommended by Becque et al. [10] are presented in Table 2 to be used with different stainless steel grades. The values used in AISI S100 are also included in the table.

Table 2. DSM parameters for distortional buckling.

	C_1	C_2	C_3	C_4	$\lambda_{d,lim}$
Austenitic steels [10]	0.80	0.15	1.1	2.2	0.533
Ferritic steels [10]	0.90	0.20	1.1	2.2	0.533
AISI S100	1.00	0.25	1.2	2.4	0.561
AS/NZS 4600	1.00	0.22	1.0	2.0	0.673

3.3 Modified Direct Strength Method

The method by Becque et al. [10] was further improved for the low slenderness range by Rossi and Rasmussen [16].

(a) Local buckling

The calculation of local buckling (without overall buckling interaction) in Eq. (19) is, however, valid only with the limit member slenderness of 0,474 for AS/NZS rules (Table 2).

$$f_l = \left[\left(1 - 2{,}11\lambda_l\right)\left(\frac{f_u}{f_y} - 1\right)\right] f_y \quad for\ \lambda_l \leq \lambda_{l,\lim}. \tag{19}$$

(b) Local-overall buckling interaction

The modification of overall buckling reduction of AS/NZS rules (Eqs. (2), (3) and (5)) is recommended in the case of overall and local buckling interaction (see Eqs. (20) and (21)). No further modification is then needed and the Eq. (15) can be used in its original form.

$$\chi = \left(1 - \frac{\bar{\lambda}}{\bar{\lambda}_{\lim}}\right)\left(\frac{f_u}{f_y} - 1\right) + 1 \quad for\ \bar{\lambda} \leq \bar{\lambda}_{\lim}. \tag{20}$$

$$\bar{\lambda}_{\lim} = \bar{\lambda}_0^{-1/\beta} + \bar{\lambda}_1. \tag{21}$$

(c) Distortional buckling

The modified formula for distortional buckling (Eq. (18)) can be used for both, austenitic and ferritic steels (see Eq. (22)).

$$f_d = \left[\left(1 - 1{,}88\lambda_d\right)\left(\frac{f_u}{f_y} - 1\right)\right] f_y \quad for\ \lambda_d \leq \lambda_{d,\lim}. \tag{22}$$

4 Elastic buckling solutions

Presented methods rely on the knowledge of elastic buckling critical stress or critical load. While manual methods for overall buckling of members are successfully used in member design for many decades, the elastic buckling solutions for local or distortional buckling of cross-sections are more complex phenomena and usually require numerical approach.

4.1 Finite Element Method

Cold-formed members are usually modelled using finite shell elements that are supported by most of the commercial FE solvers. The finite element model has to be prepared carefully taking into account proper element type, its shape function, mesh size and element aspect ratio. The benchmark test with different settings is often recommended before the final FE analysis.

The elastic buckling can be then solved by the linear eigenvalue analysis (LEA), searching for the elastic critical loads. This method, however, cannot distinguish between local, distortional and overall modes unless special constraints are included in the model. Moreover, the number of required eigenmodes is not known before the desired failure is reached. Designers usually have to calculate many values and then search manually for the first applicable buckling mode.

It is possible to suppress local and distortional buckling modes in the buckling analysis by stiffening each cross section with membrane elements [17]. This function is not usually available in FE programs, but it was recently implemented in the Abaqus plug-in developed in VTT [18]. Multipoint constraints were used to prevent overall and distortional modes by Kumar and Kalyanaraman [19]. Such approaches can greatly help the designers with selection of the proper buckling mode because the desired eigenvalue is usually the first one calculated.

In our study we used Abaqus solver [20] and S9R5 quadratic thin shell elements with reduced integration, which proved to provide acceptable results and their shape function is suitable also for modelling of cold-formed corners.

4.2 Finite Strip Method

The method particularly suitable for identifying cross-sectional critical loads is implemented in several commercial and open-source software products. It is very fast and it can generate so called signature curve, where the minimum critical loads for local or distortional buckling may be identified easily. There are several similarities with the FEM especially in the modelling phase. Cross-section has to be properly partitioned and at least two elements per face are recommended. The corner areas may require finer mesh as well as in FEM calculations.

In our study we used open-source software CUFSM [21]. The handling of inputs and outputs was automated by the Python script using the Matlab import/export module.

4.3 Generalized Beam Theory

The GBT is relatively new method and only the limited selection of programs using GBT is available. One example is GBTUL software. Even though the method is not used in this report, we encourage readers to read additional information about this theory [22, 23].

4.4 Manual methods

The closed-form solutions are usually very efficient and simple to use. They do not require special software and even though these methods provide conservative results they are very popular in engineering community and form the basic structure of current design codes. The manual methods are discussed in more detail in Appendix B.

5 Virtual buckling tests

Finite element models were used to simulate the buckling experiments on cold-formed lipped channels. The problem of additional bending effect due to the shift of effective centroid in singly symmetric sections was solved by fixing the model ends as recommended in [24]. Therefore the real length L of tested columns was always two times higher than the critical buckling length in flexural and torsional buckling ($L_{cr} = L_{cr,x} = L_{cr,y} = L_{cr,T} = ½\ L$).

5.1 Cross-sections and material

The cross-sectional shapes were designed to fail in overall torsional-flexural buckling (Section A) and flexural buckling (Section B) as in Figure 1 and Table 4. Section B was also designed to slightly violate DSM limits of the pre-qualified sections (Table 4 and Appendix A) to study the effect of long and slender element (the lip) on the critical section load. The average corner radius is 3 mm.

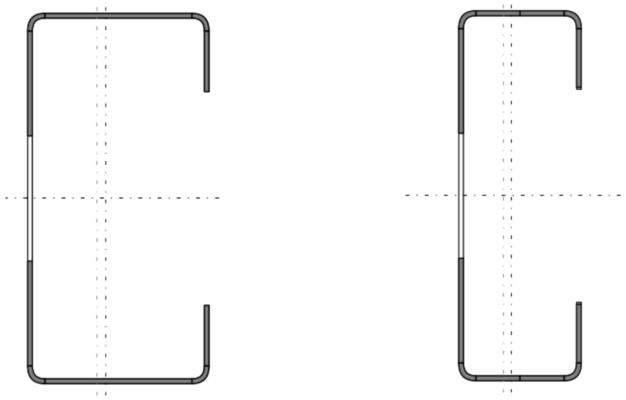

Figure 1. Studied cross-sections: Section A (left) and Section B (right).

Table 3. Cross-sectional parameters.

	h_0	b_0	D	θ	t
Section A	72 mm	36 mm	15 mm	90°	0.5 to 1.5 mm
Section B	72 mm	24 mm	15 mm	90°	0.5 to 1.5 mm

The finite element method was using Ramberg-Osgood material model [7] with the n factor equal to 10, yield strength f_y = 250 MPa and the initial modulus of elasticity E_0 = 200 GPa.

Table 4. Geometric and material limits for the use with AISI, ASCE and AS/NZS standards.

	Section A	Pre-qualified		Section B	Pre-qualified	
		column	beam		column	beam
h_0/t	48 to 144	OK	OK	48 to 144	OK	OK
b_0/t	24 to 72	OK	OK	16 to 48	OK	OK
D/t	10 to 30	OK	OK	10 to 30	OK	OK
h_0/b_0	2	OK	OK	3	OK	OK
D/b_0	0.41	OK	OK	0.62	-	OK
θ	90°	OK	OK	90°	OK	OK
E/f_y	800	OK	OK	800	OK	OK

5.2 Initial imperfections

The ultimate loads recorded in Table 5 and Table 6 are produced by the virtual testing tool [18], where the initial imperfections were combined from the overall and local component. The distribution of overall and local imperfection was provided by the tool automatically from the linear eigenvalue analysis. The magnitude of overall imperfections was L/1500 in case of columns failing in overall buckling or local-overall interaction. In the case of local imperfections, we used Dawson and Walker's formula [25] in Equation (23), where t is the plate thickness, σ_{cr} is the plate critical stress and σ_{02} is the 0,2% offset yield strength of the material.

$$w_0 = 0,023t\left(\sigma_{02}/\sigma_{cr}\right) \tag{23}$$

It should be noted that the amplitude of overall imperfections may be unproportionally higher than of local imperfections even for short columns where the local buckling is clearly dominating. However, the design codes do not provide guidance about the limit column lengths for local-overall interaction. Therefore we have reduced the overall amplitude proportionally to the critical stress ratio $\sigma_{cr}/\ \sigma_{cr,l}$ of the member and the cross-section in the case of short columns.

5.3 Ultimate loads

(a) columns failing in overall torsional-flexural buckling

Table 5. Ultimate loads (in kN) of FEM Section A in compression.

L_{cr}	t (mm)				
(mm)	0.5	0.75	1.0	1.25	1.5
125	9.692	20.455	33.452	43.821	59.494
250	9.409	20.319	30.794	43.730	59.118
500	9.673	18.498	29.609	43.266	52.642
750	9.394	19.458	29.097	39.928	48.085
1000	9.525	18.313	27.757	35.018	42.340
1250	8.811	16.131	23.328	29.507	35.996
1500	7.573	13.541	18.509	23.918	29.736
2000	4.699	8.399	11.780	15.538	19.777
3000	2.718	4.963	6.984	9.265	10.801

(b) columns failing in overall flexural buckling

Table 6. Ultimate loads (in kN) of FEM Section B in compression.

L_{cr} (mm)	t (mm) 0.5	0.75	1.0	1.25	1.5
125	9.393	17.991	26.771	35.845	50.860
250	9.136	17.392	25.578	34.487	48.640
500	9.009	15.932	24.470	32.706	42.902
750	8.230	14.267	23.060	30.158	36.800
1000	7.001	12.474	19.030	24.888	30.299
1250	4.600	n/a	14.362	n/a	23.586
1500	4.389	n/a	10.636	n/a	16.357
2000	2.719	n/a	6.492	n/a	9.767
3000	1.244	n/a	2.992	n/a	4.497

6 Comparison of the design methods

The following four methods are compared in this document:

CSM — The continuous strength method in its latest form [26] is used only for section resistance calculations since it does not cover overall buckling.

EN 1993-1-1 — The calculation of resistance of carbon steel members resistance. It is also based on EN 1993-1-3 and EN 1993-1-5.

EN 1993-1-4 — The standard procedure for calculation of stainless steel member resistance is the modification of the EN 19993-1-1 method. It uses specific member buckling curves, section classification limits and reduction factor for local buckling.

EN Talja and Salmi — The calculation of local-overall buckling interaction according to EN 1993-1-4 method is modified so that the full section area is used in the member buckling reduction and real stress is used in the effective section calculation as recommended by Talja and Salmi [9].

DSM-EN — Direct strength method recommended by Becque et al. (for ferritic stainless steels) combined with EN 1993-1-4 member buckling curves. The critical stress of the cross-section is calculated manually.

DSM-EN-FSM — Direct strength method recommended by Becque et al. combined with EN 1993-1-4 overall buckling curves. The critical stress for local and distortional buckling is obtained from CUFSM software [27]. This method was used only in member resistance calculations for selected cross-sections and variable member length.

The design methods were compared with the results of the FEM study. Because of the relatively short calculation times, the member lengths and material thicknesses were varying continuously in small steps to achieve smooth curves as results. The lengths of studied columns were from 50 to 4000 mm and the material thicknesses were from 0.5 to 2.0 mm. The material model was assumed elastic-plastic with the *n* factor equal to 10. Modulus of elasticity of 200 GPa and yield strength of 250 MPa were applied. For the CSM method, the material model was extended to a bi-linear form with the ultimate strength of 350 MPa.

The following sections show the results of this parametric study as member resistances plotted against (a) critical length or (b) material thickness. The same graphs are also presented in the nondimensional form, where the resistances divided by cross-sectional resistance Af_y are plotted against (a) member slenderness or (b) section slenderness. Design methods are compared to the FEM results (red markers in Figure 2 to Figure 11). The points named “local-overall interaction” indicate the critical length or the thickness, where the overall critical stress is equal to the local buckling critical stress.

6.1 Section A results

(a) Columns with variable length and fixed thickness to 0.5, 1.0 and 1.5 mm

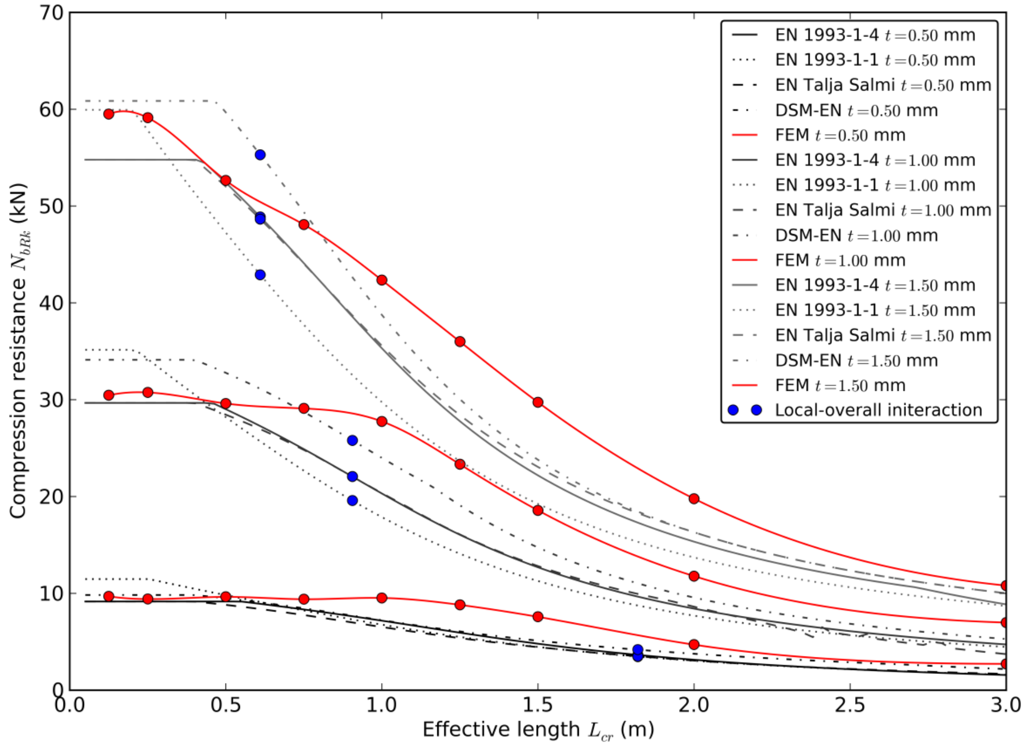

Figure 2. Compression resistance of Section A with variable length.

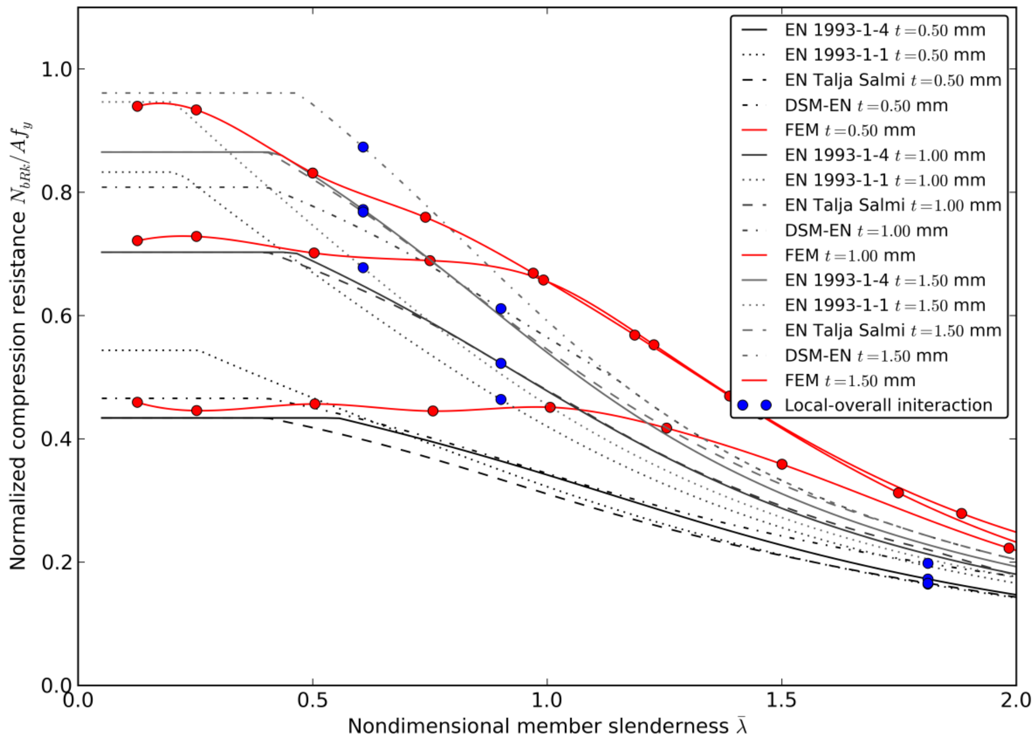

Figure 3. Nondimensional compression resistance of Section A with variable member slenderness.

(b) Columns with variable thickness and fixed length to 0.5, 0.75 and 1.0 m

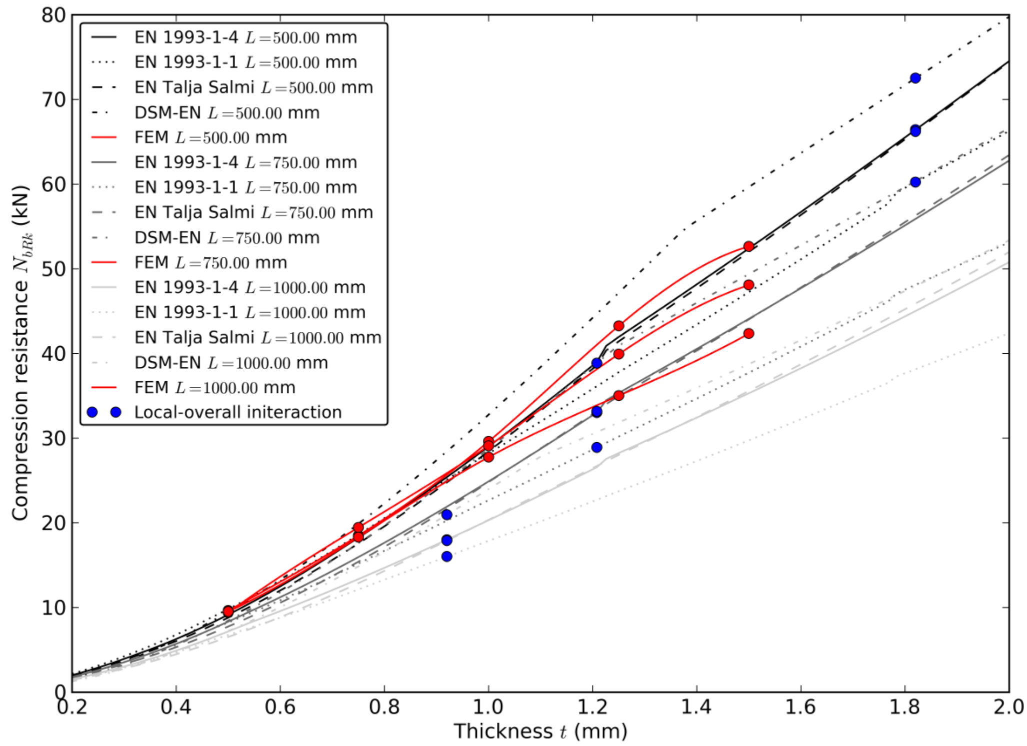

Figure 4. Compression resistance of Section A with variable thickness.

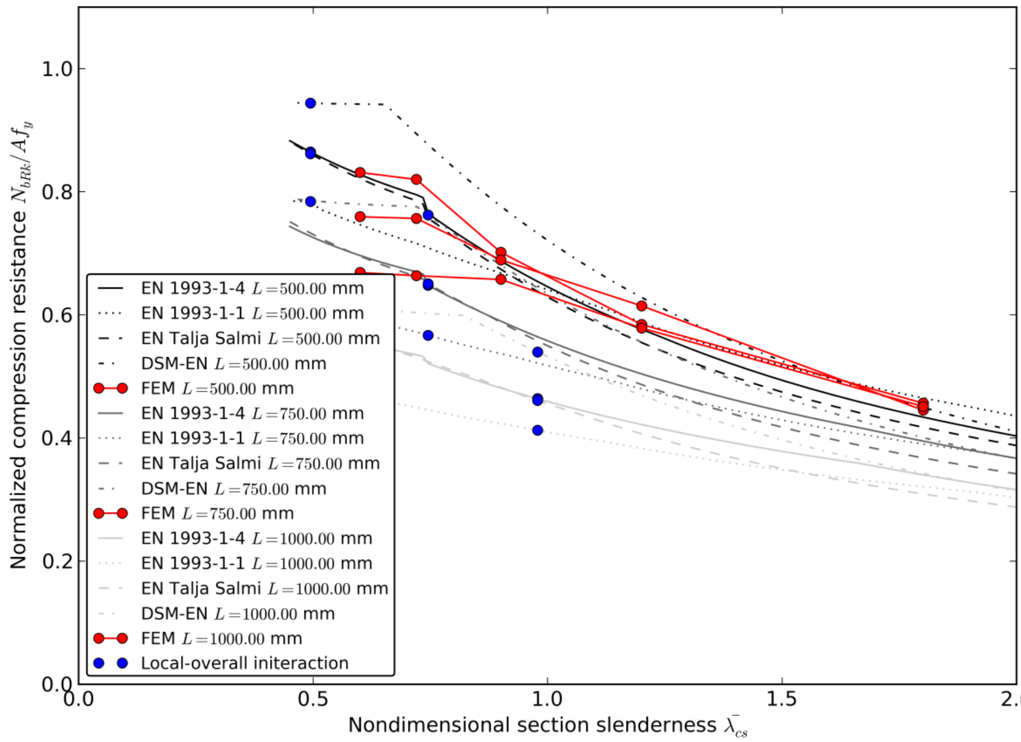

Figure 5. Nondimensional compression resistance of Section A with variable section slenderness.

(c) Comparison to FEM results

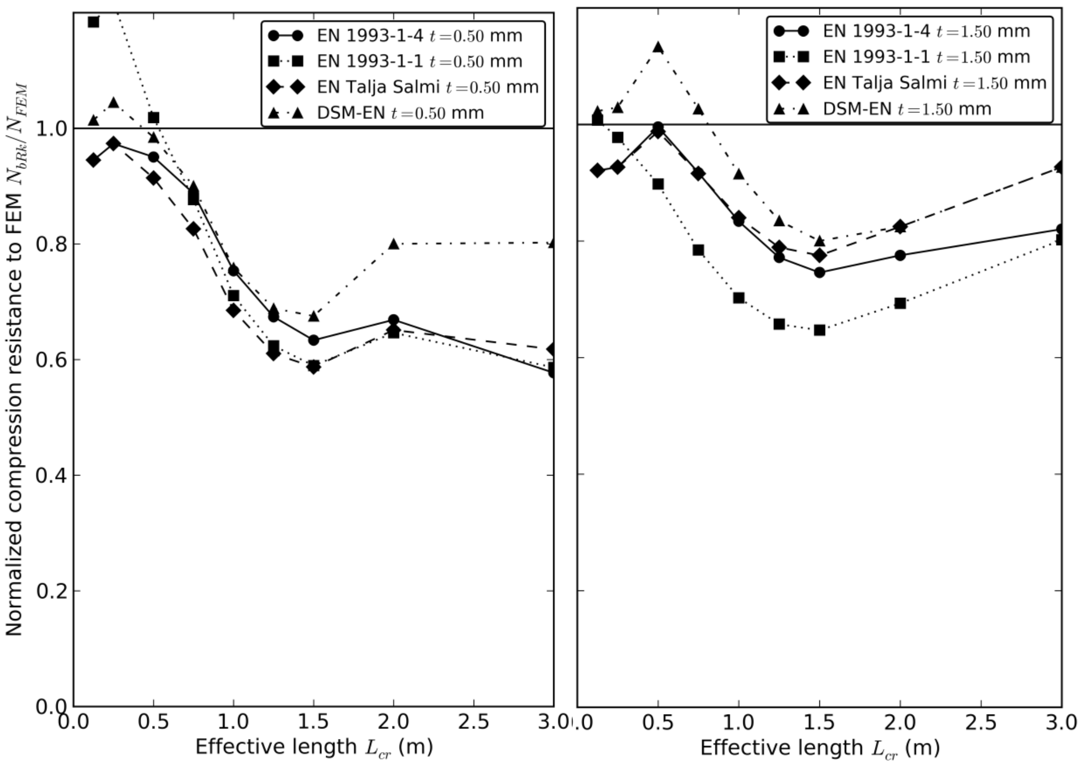

Figure 6. Compression resistance normalized to FEM results with respect to the variable length.

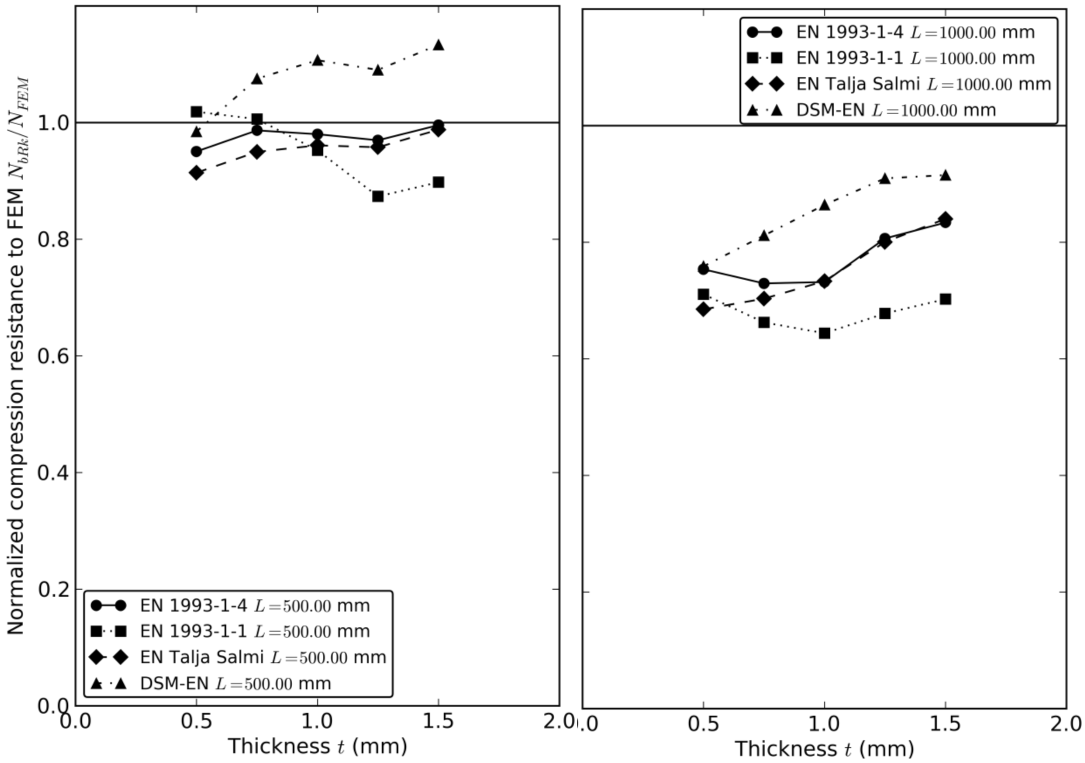

Figure 7. Compression resistance normalized to FEM results with respect to the variable thickness.

6.2 Section B results

(a) Columns with variable length and fixed thickness to 0.5, 1.0 and 1.5 mm

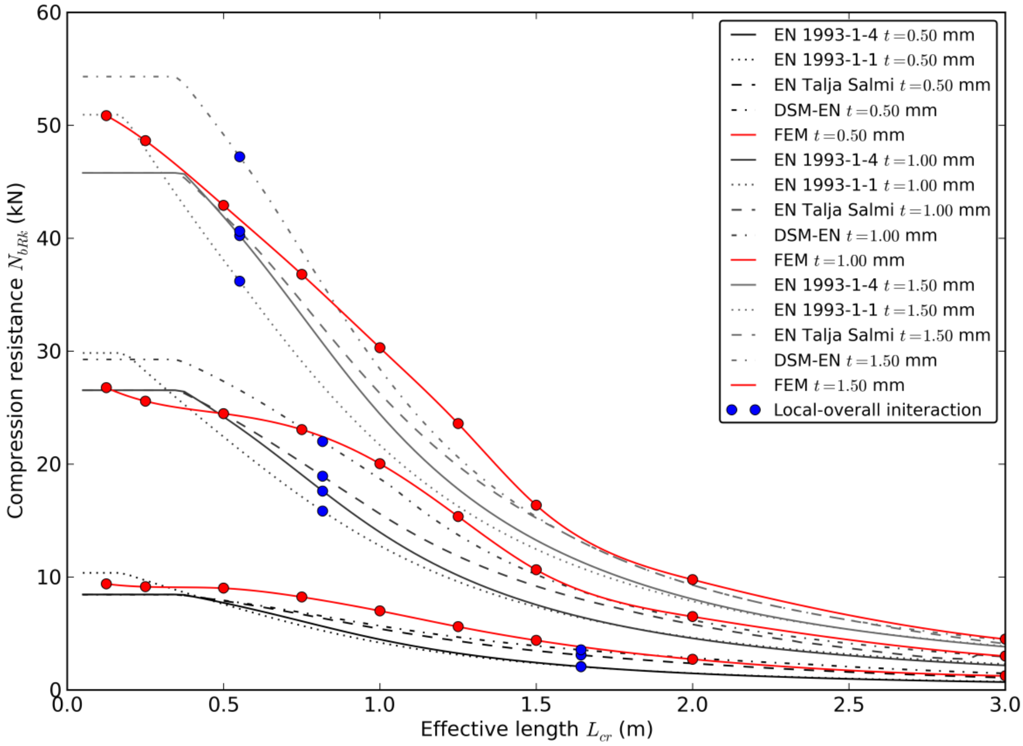

Figure 8. Compression resistance of Section B with variable length.

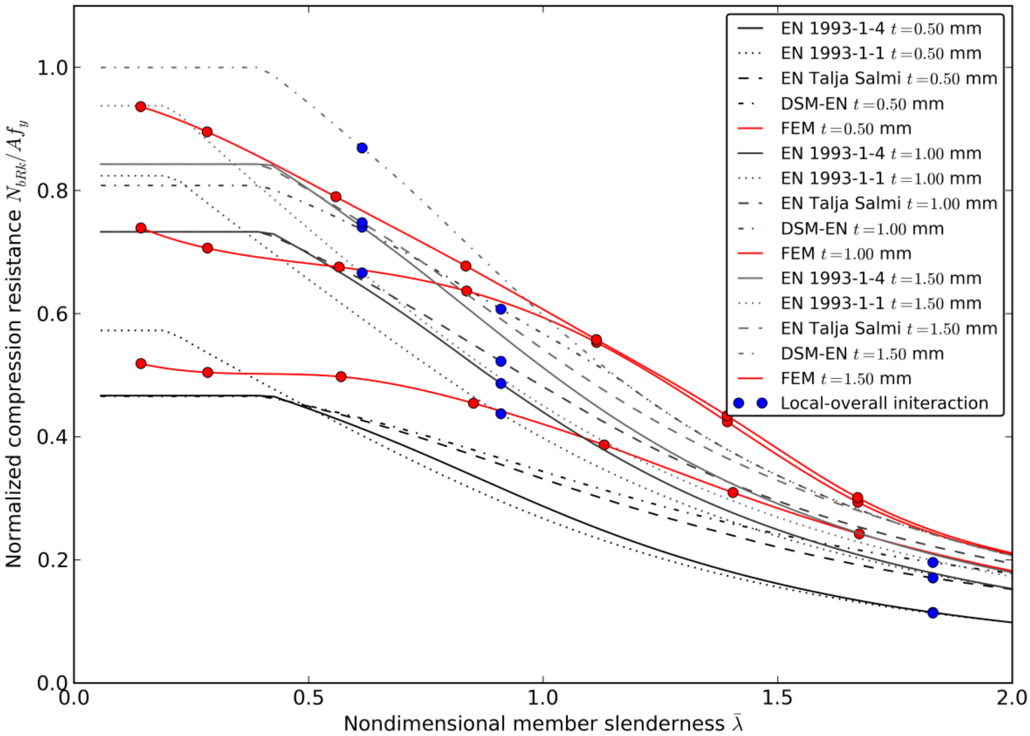

Figure 9. Nondimensional compression resistance of Section B with variable member slenderness.

(b) Columns with variable thickness and fixed length to 0.5, 0.75 and 1.0 m

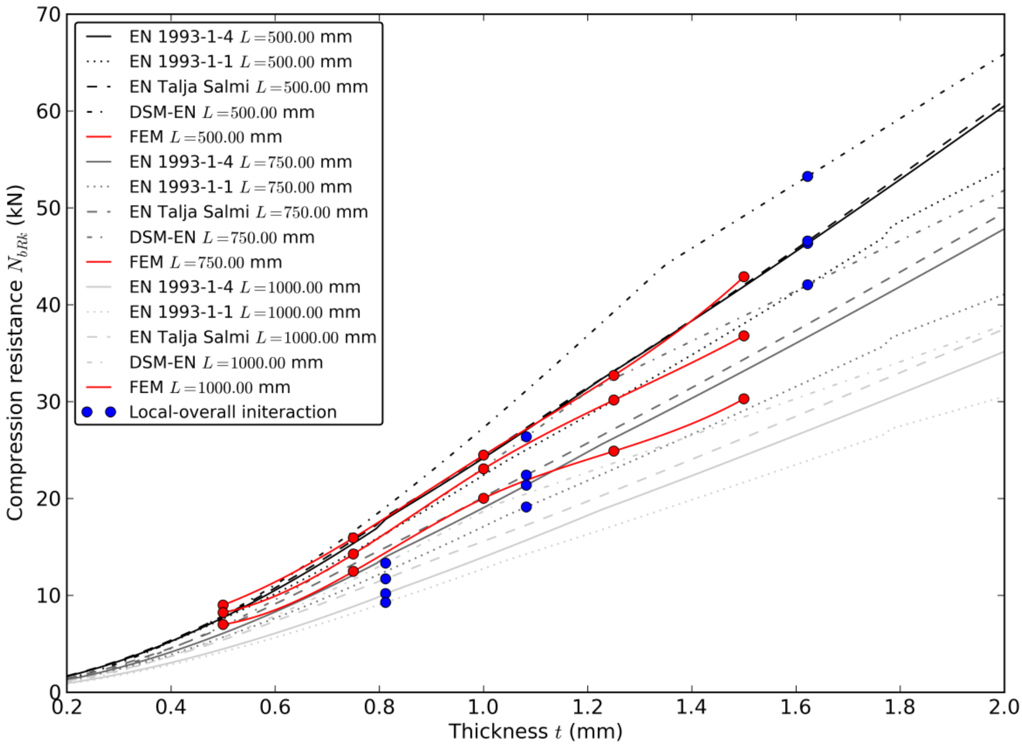

Figure 10. Compression resistance of Section B with variable thickness.

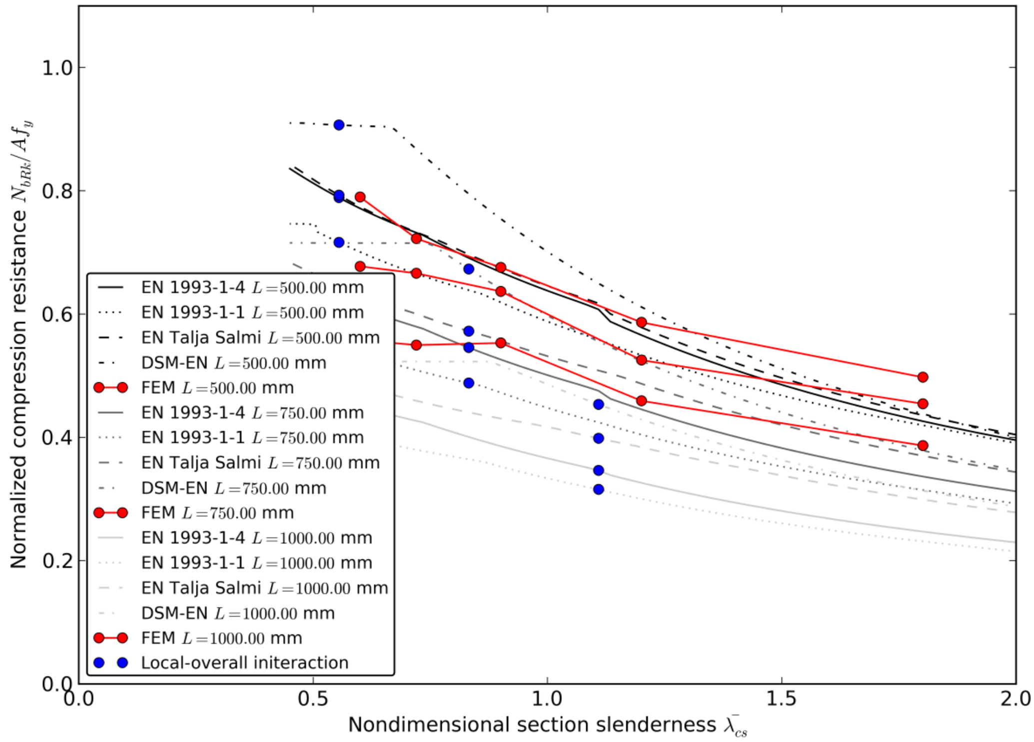

Figure 11. Nondimensional compression resistance of Section B with variable section slenderness.

(c) Comparison to FEM results

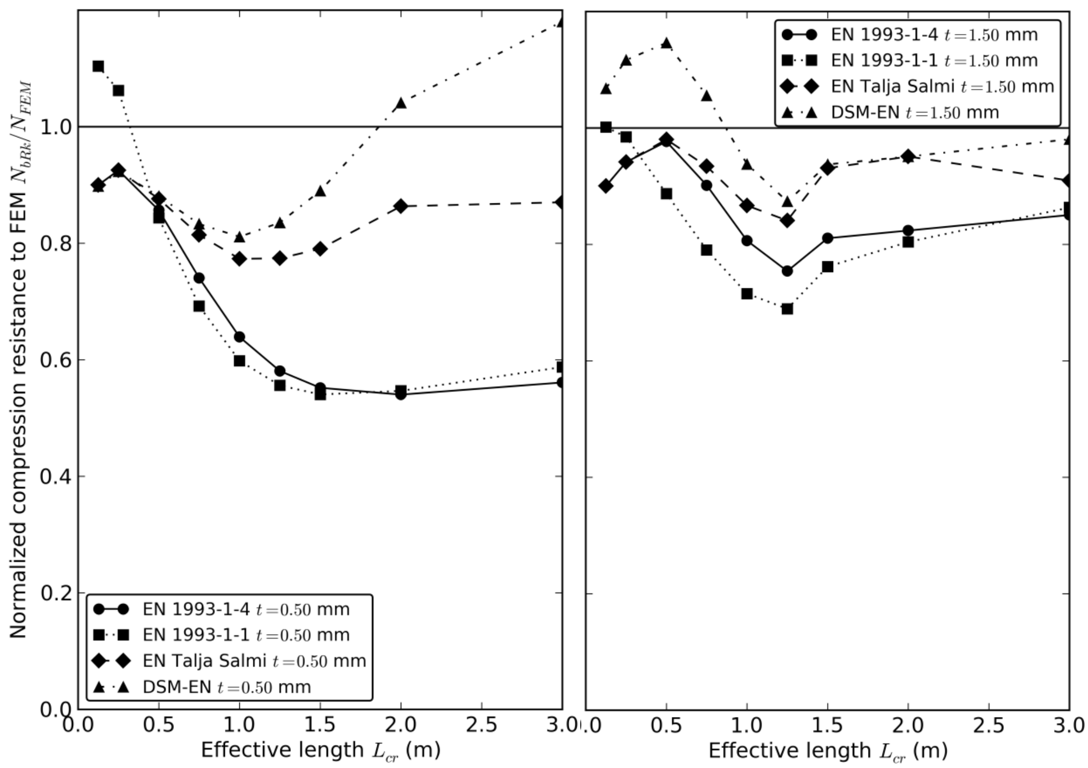

Figure 12. Compression resistance normalized to FEM results with respect to the variable length.

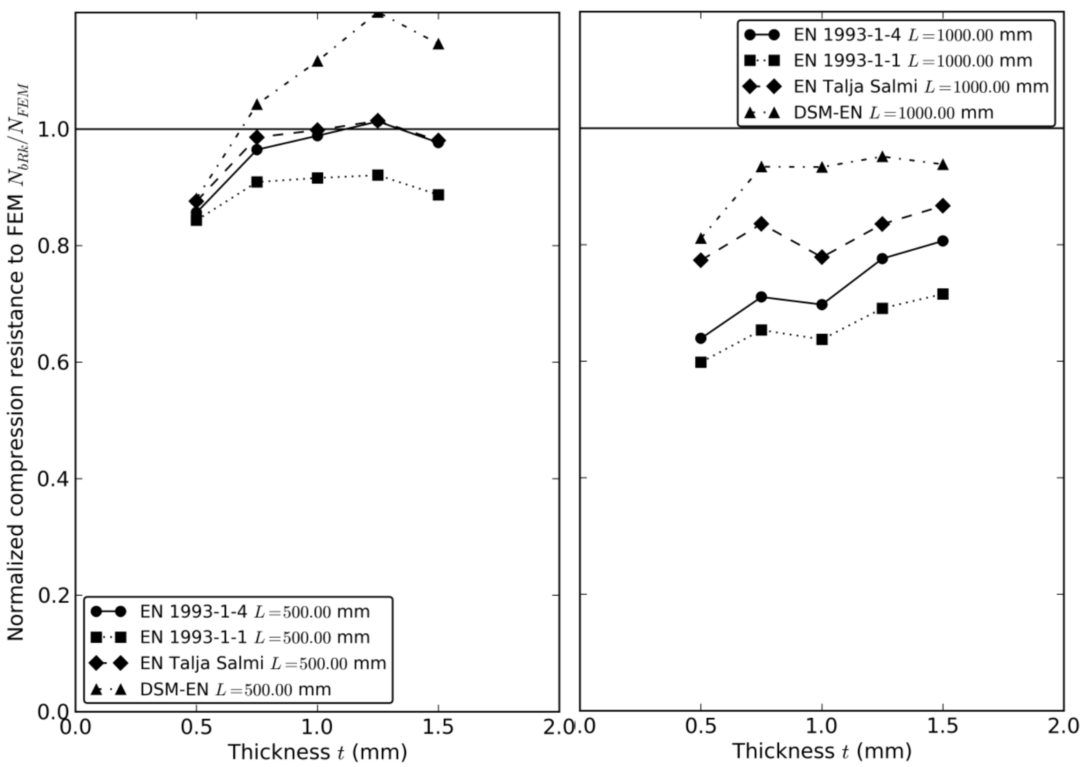

Figure 13. Compression resistance normalized to FEM results with respect to the variable thickness.

7 Discussion

Results show that the DSM method did not show significantly better results in comparison to the existing effective width method (see Figure 6 and Figure 12). However, both seem to be slightly over-predicting the member capacity in very short columns and tend to be more conservative with the increasing length (see Figure 7 and Figure 13). This effect can be caused by unnecessary reduction of sections that fail in overall buckling at low stress levels in the case of the effective section calculation. It was partly eliminated by applying the approach from AISI and AS/NZS standards recommended by Talja and Salmi. Smaller thicknesses are somewhat more conservative compared to the FEM results.

8 Conclusions

8.1 Effective Width Method

The plate slenderness calculation in EN 1993-1-4, Section 5.2.3 is based on stress equal to the material yield strength f_y. We recommend that the modification of the calculation should be considered, which takes into account the overall buckling stress of the full cross section (as it is used in AISI, ASCE and AS/NZS standards and as it is recommended by Talja and Salmi). The modified formula is presented in Eq. (24). The full cross-section shall be used in overall buckling calculation of the reduction factor χ.

$$\bar{\lambda}_p = \sqrt{\chi}\,\frac{\bar{b}/t}{28.4\varepsilon k_\sigma}. \tag{24}$$

8.2 Direct Strength Method

The application of DSM in the member design does not provide significant improvement in the accuracy of results, but it is easier and more straightforward than the effective width and effective thickness calculations which usually need several iterations and are limited to simple cross-sections. The use of DSM is also limited to certain sectional shapes and loading combinations but its range can be extended by calibration without the need of more complex design rules.

DSM tends to be too conservative for sections with one part remarkably more slender than others (such as top hat sections with long unstiffened lips).

The main drawback of DSM use is the need of FSM or FEM software providing the accurate prediction of critical stress of local or distortional buckling. In that sense, a proper FEM analysis will produce much more accurate resistance prediction directly without the need of any further calculations.

Eurocode 3, Part 1-5 provides rules for calculation of local buckling elastic critical stress of plated elements, which can serve as a basis for manual calculation of cross-sectional local buckling critical stress. Moreover, the rules for distortional buckling critical stress of edge stiffeners are present in Eurocode 3, Part 1-3, and therefore the basic values of DSM are readily available in the code, so that the implementation of DSM method is possible. From the modified DSM rules recommended by Rossi and Rasmussen [16], only the distortional buckling calculation can be adapted into the Eurocode because the local and local-overall buckling resistances are related only to the AS/NZS rules in the presented form.

9 Recommendations

DSM stands between traditional design methods and more sophisticated numerical methods such as FEM, and it yields best results in its semi-numerical form, where critical stresses from FSM, FEM or other numerical simulations are used. Due to many limitations explained here or in the Design Guide [28], we do not recommend the method to be used in Eurocode since nowadays FEM calculations provide more realistic predictions with reasonable computational time. If the DSM is considered as appendix to EN 1993-1-4, the following issues should be taken into account:

1) Eurocode provides closed-form solutions of elastic buckling of plates (local buckling) and stiffeners (distortional buckling) that may be linked to the DSM.

2) If a numerical solution of elastic buckling is recommended, its algorithm should be reviewed. We recommend CUFSM, an open-source (Academic Free Licence) algorithm provided by Ben Schafer, which was used in this report.

3) Parameters of DSM curves have to be calibrated. The work by Becque et al. [10] provides one recommendation that may be used if it satisfies the reliability criteria.

4) The applicability of pre-qualified cross-section limits should be checked, because of the Eurocode specific rules for local and distortional critical stresses and overall buckling reduction factors.

References

[1] Hancock, G.J., Kwon, Y.B. & Stefan Bernard, E. Strength design curves for thin-walled sections undergoing distortional buckling. Journal of Constructional Steel Research 1994, Vol. 31, No. 2-3, pp. 169–186. ISSN 0143-974X. doi: DOI: 10.1016/0143-974X(94)90009-4.

[2] Schafer, B.W. & Peköz, T. Direct strength prediction of cold-formed steel members using numerical elastic buckling solutions. 14th International Specialty Conference on Cold-Formed Steel Structures. St. Louis, Missouri U.S.A., October 15–16, 1998. 1998.

[3] Schafer, B. Local, Distortional, and Euler Buckling of Thin-Walled Columns. Journal of Structural Engineering 2002, 03/01; 2013/03, Vol. 128, No. 3, pp. 289–299. ISSN 0733-9445. doi: 10.1061/(ASCE)0733-9445(2002)128:3(289). http://dx.doi.org/10.1061/(ASCE)0733-9445(2002)128:3(289).

[4] Schafer, B.W. Review: The Direct Strength Method of cold-formed steel member design. Journal of Constructional Steel Research 2008, 8, Vol. 64, No. 7–8, pp. 766–778. ISSN 0143-974X. doi: DOI: 10.1016/j.jcsr.2008.01.022.

[5] VTT-R-04651-12. Hradil, P., Talja, A., Real, E. & Mirambell, E. SAFSS Work Package 2: Review of available data. Espoo, Finland: VTT Technical Research Centre of Finland, 2012.

[6] Ayrton, W.E. & Perry, J. On struts. The Engineer 1886, Vol. 62, pp. 464–465.

[7] Technical Note No. 902. Ramberg, W. & Osgood, W.R. Description of stress-strain curves by three parameters. Washington, D.C., USA: National Advisory Committee for Aeronautics, 1943.

[8] Hradil, P., Fülöp, L. & Talja, A. Global stability of thin-walled ferritic stainless steel members. Thin-Walled Structures 2012, 12, Vol. 61, No. 0, pp. 106–114. ISSN 0263-8231. doi: 10.1016/j.tws.2012.05.006.

[9] VTT Publications 201. Talja, A. & Salmi, P. Simplified design expressions for cold-formed channel sections. Espoo, Finland: VTT Technical Research Centre of Finland, 1994.

[10] Becque, J., Lecce, M. & Rasmussen, K.J.R. The direct strength method for stainless steel compression members. Journal of Constructional Steel Research 2008, 11, Vol. 64, No. 11, pp. 1231–1238. ISSN 0143-974X. doi: DOI: 10.1016/j.jcsr.2008.07.007.

[11] Pham, C. & Hancock, G. Direct Strength Design of Cold-Formed C-Sections for Shear and Combined Actions. Journal of Structural Engineering

2012, 06/01; 2013/03, Vol. 138, No. 6, pp. 759–768. ISSN 0733-9445. doi: 10.1061/(ASCE)ST.1943-541X.0000510. http://dx.doi.org/10.1061/(ASCE)ST.1943-541X.0000510.

[12] Research Report No R821. Bezkorovainy, P., Burns, T. & Rasmussen, K.J.R. Strength Curves for Metal Plates in Compression. Sydney, Australia: Centre for Advanced Structural Engineering, Department of Civil Engineering, The University of Sydney, 2002.

[13] Johnson, A. & Winter, G. Behaviour of Stainless Steel Columns and Beams. Journal of Structural Engineering 1966, Vol. 92(ST5), pp. 97–118.

[14] AISI S100-2007 North American Specification for the Design of Cold-Formed Steel Structural Members. Washington DC: 2007.

[15] AISI S100-2007-C Commentary on North American Specification for the Design of Cold-Formed Steel Structural Members. Washington DC: 2007.

[16] Rossi, B. & Rasmussen, K. Carrying Capacity of Stainless Steel Columns in the Low Slenderness Range. Journal of Structural Engineering 2012, 05/28; 2013/02, pp. 502. ISSN 0733-9445. doi: 10.1061/(ASCE)ST.1943-541X.0000666. http://dx.doi.org/10.1061/(ASCE)ST.1943-541X.0000666.

[17] Zhang, L. & Tong, G.S. Lateral buckling of web-tapered I-beams: A new theory. Journal of Constructional Steel Research 2008, 12, Vol. 64, No. 12, pp. 1379–1393. ISSN 0143-974X. doi: DOI: 10.1016/j.jcsr.2008.01.014.

[18] Hradil, P., Fülöp, L. & Talja, A. Virtual testing of cold-formed structural members. Rakenteiden Mekaniikka (Journal of Structural Mechanics) 2011, Vol. 44, No. 3, pp. 206–217. ISSN 0783-6104.

[19] Kumar, M. & Kalyanaraman, V. Design Strength of Locally Buckling Stub-Lipped Channel Columns. Journal of Structural Engineering 2012, 11/01; 2013/03, Vol. 138, No. 11, pp. 1291-1299. ISSN 0733-9445. doi: 10.1061/(ASCE)ST.1943-541X.0000575. http://dx.doi.org/10.1061/(ASCE)ST.1943-541X.0000575.

[20] ABAQUS User Manual (version 6.11). Pawtucket, RI, USA: Hibbitt, Karlsson & Sorensen Inc., 2011.

[21] Schafer, B.W., Li, Z. & Moen, C.D. Computational modeling of cold-formed steel. Thin-Walled Structures 2010, 11, Vol. 48, No. 10–11, pp. 752–762. ISSN 0263-8231. doi: DOI: 10.1016/j.tws.2010.04.008.

[22] Silvestre, N. & Camotim, D. Distortional buckling formulae for cold-formed steel C and Z-section members: Part I – derivation. Thin-Walled Structures 2004, 11, Vol. 42, No. 11, pp. 1567–1597. ISSN 0263-8231. doi: DOI: 10.1016/j.tws.2004.05.001.

[23] Dinis, P.B., Camotim, D. & Silvestre, N. GBT formulation to analyse the buckling behaviour of thin-walled members with arbitrarily 'branched' open cross-sections. Thin-Walled Structures 2006, 1, Vol. 44, No. 1, pp. 20–38. ISSN 0263-8231. doi: DOI: 10.1016/j.tws.2005.09.005.

[24] Rasmussen, K.J.R. & Hancock, G.J. Design of Cold-Formed Stainless Steel Tubular Members. I: Columns. Journal of Structural Engineering 1993, August 1993, Vol. 119, No. 8, pp. 2349–2367. doi: 10.1061/(ASCE)0733-9445(1993)119:8(2349).

[25] Dawson, R.G. & Walker, A.C. Post-Buckling of Geometrically Imperfect Plates. Journal of the Structural Division ASCE 1972, Vol. 98, No. 1, pp. 75–94.

[26] Afshan, S. & Gardner, L. The continuous strength method for structural stainless steel. Stainless Steel in Structures, 4th International Experts Seminar. Ascot, UK, 6.–7.12.2012. 2012.

[27] Li, Z. & Schafer, B.W. Buckling analysis of cold-formed steel members with general boundary conditions using CUFSM: conventional and constrained finite strip methods. Twentieth International Specialty Conference on Cold-Formed Steel Structures. Saint Louis, Missouri, USA, 3–4 November 2010. 2010.

[28] AISI(ed.). Direct Strength Method (DSM) Design Guide. Washington, DC: American Iron and Steel Institute, 2006. Design Guide CF06-1.

Appendix A: DSM limits for pre-qualified members

The geometrical and material limits in both standards (AISI S100:2007 and AS/NZS 4600:2005) are generally very similar, only small differences are highlighted in Table 7, Table 8, Table 9 and Table 10.

Table 7. Pre-qualified columns (Part 1/2).

<table>
<tr><th>Sections
in compression</th><th>AISI S100 limits</th><th>AS/NZS 4600 limits</th></tr>
<tr><td>Lipped channels
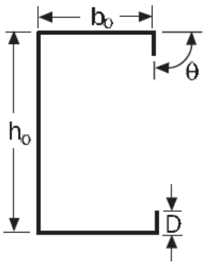</td><td colspan="2">$h_0/t < 472$
$b_0/t < 159$
$4 < D/t < 33$
$0{,}7 < h_0/b_0 < 5$
$0{,}05 < D/b_0 < 0{,}41$
$\theta = 90°$
$E/f_y > 340\,(f_y < 593\,MPa)$</td></tr>
<tr><td>Complex lips of
lipped channels
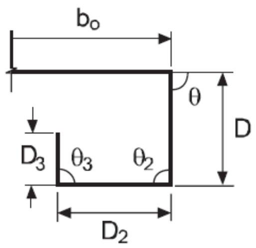</td><td>$D_2/t < 34$
$D_2/D < 2$
$D_3/t < 34$
$D_3/D < 1$</td><td>not applicable</td></tr>
<tr><td>Lipped channels with
web stiffener(s)
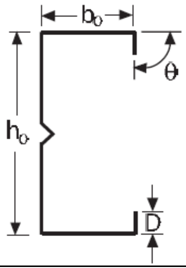</td><td colspan="2">$h_0/t < 489$
$b_0/t < 160$
$6 < D/t < 33$
$1{,}3 < h_0/b_0 < 2{,}7$
$0{,}05 < D/b_0 < 0{,}41$
max. 2 stiffeners
$E/f_y > 340\,(f_y < 593\,MPa)$</td></tr>
<tr><td>Z-section
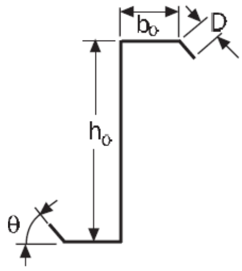</td><td colspan="2">$h_0/t < 137$
$b_0/t < 56$
$0 < D/t < 36$
$1{,}5 < h_0/b_0 < 2{,}7$
$0 < D/b_0 < 0{,}73$
$\theta = 50°$
$E/f_y > 590\,(f_y < 345\,MPa)$</td></tr>
</table>

Table 8. Pre-qualified columns (Part 2/2).

<table>
<tr><th>Sections
in compression</th><th>AISI S100 limits</th><th>AS/NZS 4600 limits</th></tr>
<tr><td>Rack upright
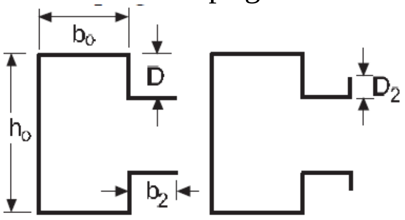
</td><td>See Lipped channel with complex lips</td><td>$h_0/t < 51$
$b_0/t < 22$
$5 < D/t < 8$
$2{,}1 < h_0/b_0 < 2{,}9$
$1{,}6 < b_2/D < 2{,}0$
$D_2/h_0 = 0{,}3$
$\theta = 50°$
$E/f_y > 340\,(f_y < 593\ MPa)$</td></tr>
<tr><td>Hat
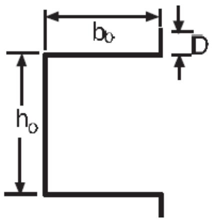
</td><td colspan="2">$h_0/t < 50$
$b_0/t < 20$
$4 < D/t < 6$
$1 < h_0/b_0 < 1{,}2$
$D/b_0 = 0{,}13$
$\theta = 50°$
$E/f_y > 428\,(f_y < 476\ MPa)$</td></tr>
</table>

Table 9. Pre-qualified beams (Part 1/2).

<table>
<tr><th>Sections
in bending</th><th>AISI S100 limits</th><th>AS/NZS 4600 limits</th></tr>
<tr><td rowspan="3">Hats (decks) with stiffened flange in compression
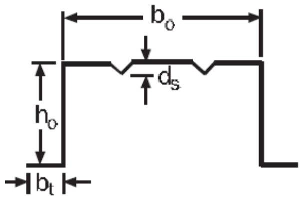
</td><td colspan="2">$h_0/t < 97$
$b_0/t < 467$
$0 < b_t/t < 26$
$0.14 < h_0/b_0 < 0{,}87$</td></tr>
<tr><td>$0{,}88 < b_0/b_t < 5{,}4$</td><td>$0{,}88 < b_0/b_t < 4$</td></tr>
<tr><td colspan="2">$E/f_y > 492\,(f_y < 414\ MPa)$</td></tr>
<tr><td>Trapezoids (decks) with stiff. flange in compression
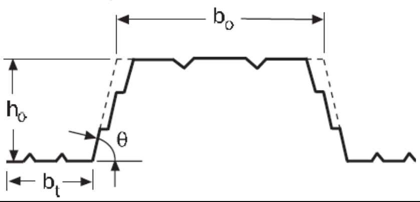
</td><td colspan="2">$h_0/t < 203$
$b_0/t < 231\ 42 < (h_0/\sin\theta)/b_0 < 1{,}91$
$1{,}1 < h_0/b_t < 3{,}38$
max. 2 stiffeners per element
$52° < \theta < 84°$
$E/f_y > 310\,(f_y < 655\ MPa)$</td></tr>
</table>

Table 10. Pre-qualified beams (Part 2/2).

Sections in bending	AISI S100 limits	AS/NZS 4600 limits
Lipped channels 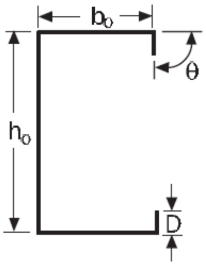	$h_0/t < 321$ $b_0/t < 75$ $0 < D/t < 34$ $1{,}5 < h_0/b_0 < 17$ $0 < D/b_0 < 0{,}7$ $44° < \theta < 90°$ $E/f_y > 421\left(f_y < 483\ MPa\right)$	
Complex lips of lipped channels 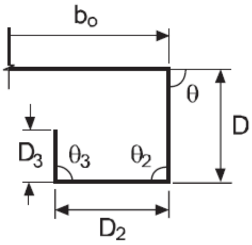	$D_2/t < 34$ $D_2/D < 2$ $D_3/t < 34$ $D_3/D < 1$	not applicable
Lipped channels with web stiffener(s) 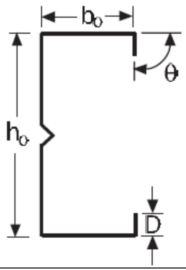	$h_0/t < 358$ $b_0/t < 58$ $14 < D/t < 17$ $5{,}5 < h_0/b_0 < 11{,}7$ $0{,}27 < D/b_0 < 0{,}56$ $\theta = 90°$ $E/f_y > 578\left(f_y < 352\ MPa\right)$	
Z-section 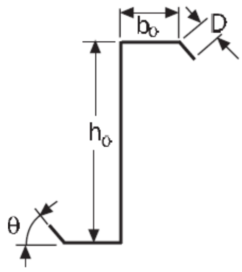	$h_0/t < 183$ $b_0/t < 71$ $10 < D/t < 16$ $2{,}5 < h_0/b_0 < 4{,}1$ $0{,}15 < D/b_0 < 0{,}34$ $36° < \theta < 90°$ $E/f_y > 440\left(f_y < 462\ MPa\right)$	$E/f_y > 400\left(f_y < 462\ MPa\right)$
Complex lips of Z-sections 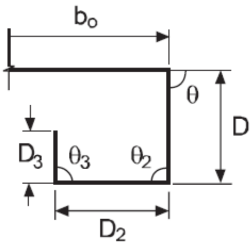	$D_2/t < 34$ $D_2/D < 2$ $D_3/t < 34$ $D_3/D < 1$	not applicable

Appendix B: Closed-form elastic buckling solutions

Local buckling

(a) element method

A conservative approach assumes that the critical elastic buckling load $\sigma_{cr,l}$ is the smallest buckling load of the cross-section plate elements $\sigma_{cr,el}$ (Eqs. (25) and (26)) with hinged corners. Alternatively, it can be calculated as the weighted average of plate critical loads which may results in higher prediction in some cases. The values t_{el} and b_{el} stand for the element thickness and width respectively. The factor k is usually 4 for intermediate and 0.425 for outstanding elements. This approach is discussed in more detail in Appendix C.

$$\sigma_{cr,l} = \min\left(\sigma_{cr,el}\right) \text{ or } \sigma_{cr,l} = \frac{\sum \sigma_{cr,el} b_{el}}{\sum b_{el}}. \tag{25}$$

$$\sigma_{cr,el} = k \frac{\pi^2 E}{12\left(1-\mu^2\right)}\left(\frac{t_{el}}{b_{el}}\right)^2. \tag{26}$$

(b) interaction method for lipped channels

More accurate prediction can be achieved by taking into account the interaction between section elements. Such methods are, however, restricted to the certain cross sections. In this example the flage-lip (*f-l*) and flange-web (*f-w*) interaction of lipped channel is calculated [3].

$$\sigma_{cr,l} = \min\left(\sigma_{cr,f-l}, \sigma_{cr,f-w}\right). \tag{27}$$

$$\begin{aligned} \sigma_{cr,f-l} &= k_{f-l} \frac{\pi^2 E}{12\left(1-\mu^2\right)}\left(\frac{t}{b_0}\right)^2 \\ \sigma_{cr,f-w} &= k_{f-w} \frac{\pi^2 E}{12\left(1-\mu^2\right)}\left(\frac{t}{b_0}\right)^2. \end{aligned} \tag{28}$$

$$\begin{aligned} k_{f-l} &= -11,07\left(\frac{D}{b_0}\right)^2 + 3,95\left(\frac{D}{b_0}\right) + 4 \quad \left(\frac{D}{b_0}\right) < 0,6 \\ k_{f-w} &= \begin{cases} 4\left[2-\left(\dfrac{b_0}{h_0}\right)^{0,4}\right]\left(\dfrac{b_0}{h_0}\right)^2 & \text{when } \left(\dfrac{h_0}{b_0}\right) \geq 1 \\ 4\left[2-\left(\dfrac{h_0}{b_0}\right)^{0,2}\right] & \text{else} \end{cases}. \end{aligned} \tag{29}$$

Distortional buckling

The manual calculation of distortional buckling in Eurocode is based on isolation of edge stiffeners that consists of section flange and lip and then calculation of their sectional properties (A_s and I_s) and rotational spring stiffness K.

$$\sigma_{cr,s} = \frac{2\sqrt{KEI_s}}{A_s}. \tag{30}$$

Similar methods are implemented in EN 1993-1-5, AS/NZS and AISI standards. The calculation of critical load of lipped C and Z sections is developed in [3]. The results can be used for DSM application or for the stiffener thickness reduction as in EN 1993.

Overall buckling

For columns subjected to overall buckling, the critical stress is always the smallest of critical stresses of all possible overall failure modes. Depending on the cross-section shape, it could be flexural buckling to y or z axis $\sigma_{E,y(z)}$, torsional buckling σ_T or torsional-flexural buckling $\sigma_{TF,y(z)}$. The support conditions are taken into account by reducing or extending the critical length to y and z axis $L_{cr,y(z)}$ and in torsion $L_{cr,T}$.

$$\sigma_{Ey(z)} = \frac{\pi^2 E}{\left(L_{cr,y(z)}/i_{y(z)}\right)^2}. \tag{31}$$

$$\sigma_T = \frac{1}{A_g i_0^2}\left(GI_t + \frac{\pi^2 EI_w}{L_{cr,T}^2}\right), \text{ where } i_0 = \sqrt{i_y^2 + i_z^2 + y_0^2 + z_0^2}. \tag{32}$$

$$\sigma_{TFy(z)} = \frac{1}{2\beta_{y(z)}}\left[\left(\sigma_{Ey(z)} + \sigma_T\right)^2 - 4\beta_{y(z)}\sigma_{Ey(z)}\sigma_T\right], \text{ where}$$
$$\beta_y = 1 - \left(z_0/i_0\right)^2 \text{ and } \beta_z = 1 - \left(y_0/i_0\right)^2. \tag{33}$$

Appendix C: Example calculations of studied cross-sections

The following calculation protocols were automatically generated by Python script producing TeX document and converted to pdf format. The idea was to provide a simple tool that is able to produce calculation protocols of most of the current design methods that can be easily applied to any cold-formed cross-sections. The resistances of Section A and Section B are calculated with effective length 1.0 m and material thickness 1.0 mm.

Compressive strength of Section A (Liped channel 72x36 mm)

Petr Hradil

March 28, 2013

Contents

1 Compression resistance according to EN 1993 rules for stainless steel

1.1 Cross-section classification

Upper lip: $c/t = 15/1.0 = 15.0 > 11.3$ Class 4
Upper flange: $c/t = 36/1.0 = 36.0 > 29.0$ Class 4
Web: $c/t = 72/1.0 = 72.0 > 29.0$ Class 4
Lower flange: $c/t = 36/1.0 = 36.0 > 29.0$ Class 4
Lower lip: $c/t = 15/1.0 = 15.0 > 11.3$ Class 4
Class 4 cross-section.

1.2 Gross cross-section

$A_{real} = 169\, mm^2$
$A_{g,sh} = \sum_{i=1}^{m} b_i ti = 174\, mm^2$
$I_{g,sh,x} = 149352\, mm^2$
$I_{g,sh,y} = 37548\, mm^2$
$\delta = 0.43 \frac{\sum_{j=1}^{n} r_j \frac{\phi_j}{90}}{\sum_{i=1}^{m} b_{p,i}} = 0.031$ (EN 1993-1-3 (5.1))
$A_g = A_{g,sh}(1 - \delta) = 174(1 - 0.031) = 169\, mm^2$
$I_{g,x} = I_{g,sh,x}(1 - 2\delta) = 149352(1 - 2 \cdot 0.031) = 140121\, mm^4$
$I_{g,y} = I_{g,sh,y}(1 - 2\delta) = 37548(1 - 2 \cdot 0.031) = 35227\, mm^4$

1.3 Effective cross-section

$\chi_d = 0.936$ after 2 iterations

1.3.1 Upper lip

$k_\sigma = 0.430$ (EN 1993-1-5, Table 4.2)
$\bar{\lambda}_p = \chi_d \frac{b/t}{28.4\epsilon\sqrt{k_\sigma}} = 0.936 \frac{14/1.0}{28.4 \cdot 0.97 \cdot \sqrt{0.4}} = 0.732$
for outstanding element $\rho = \frac{1.0}{\bar{\lambda}_p} - \frac{0.231}{\bar{\lambda}_p^2} = \frac{1.0}{0.73} - \frac{0.231}{0.73^2} = 0.935$ (EN 1993-1-4)

1.3.2 Upper flange

$k_\sigma = 4.000$ (EN 1993-1-5, Table 4.1)
$\bar{\lambda}_p = \chi_d \frac{b/t}{28.4\epsilon\sqrt{k_\sigma}} = 0.936 \frac{34/1.0}{28.4 \cdot 0.97 \cdot \sqrt{4.0}} = 0.582$
for internal element $\rho = \frac{0.722}{\bar{\lambda}_p} - \frac{0.125}{\bar{\lambda}_p^2} = \frac{0.722}{0.58} - \frac{0.125}{0.58^2} = 0.871$ (EN 1993-1-4)

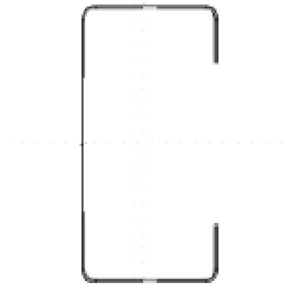

Figure 1: Effective section of Lipped channel 36.0x72.0x15.0 1.0 mm

$N_{cr,T} = \frac{1}{i_0^2}(GI_t + \frac{\pi^2 EI_w}{L_{cr,T}^2}) = \frac{1}{49.475^2}(76923 \cdot 56 + \frac{\pi^2 200000 \cdot 51567855}{1000^2}) = 43.4\ kN$
$\beta = 1 - (\frac{x_0}{r_0})^2 = 0.539$
$N_{cr,TF} = \frac{1}{2\beta}[N_{cr,T} + N_{cr,x} - \sqrt{(N_{cr,T} + N_{cr,x})^2 - 4\beta N_{cr,T} N_{cr,x}}] = 39.9\ kN$
$N_{cr} = min(N_{cr,TF}, N_{cr,y}) = 39.9\ kN$ (singly symmetric section)
$\bar{\lambda} = \sqrt{\frac{Af_y}{N_{cr}}} = \sqrt{\frac{119 \cdot 250}{39930.2}} = 0.862$
$\phi = \frac{1}{2}(1 + \alpha(\bar{\lambda} - \bar{\lambda}_0) + \bar{\lambda}^2) = \frac{1}{2}(1 + 0.49(0.86 - 0.4) + 0.86^2) = 0.985$
$\chi = \frac{1}{\phi + \sqrt{\phi^2 - \bar{\lambda}^2}} = \frac{1}{0.98 + \sqrt{0.98^2 - 0.86^2}} \leq 1\ \chi = 0.685$
$N_{b,Rk} = \chi A f_y = 0.68 \cdot 119 \cdot 250 = 20.3\ kN$

2 Compression resistance according to EN 1993 rules for carbon steel

2.1 Cross-section classification

Upper lip: $c/t = 15/1.0 = 15.0 > 13.6$ Class 4
Upper flange: $c/t = 36/1.0 = 36.0 \leq 40.7$ Class 3
Web: $c/t = 72/1.0 = 72.0 > 40.7$ Class 4
Lower flange: $c/t = 36/1.0 = 36.0 \leq 40.7$ Class 3
Lower lip: $c/t = 15/1.0 = 15.0 > 13.6$ Class 4
Class 4 cross-section.

2.2 Gross cross-section

$A_{real} = 169\, mm^2$
$A_{g,sh} = \sum_{i=1}^{m} b_i ti = 174\, mm^2$
$I_{g,sh,x} = 149352\, mm^2$
$I_{g,sh,y} = 37548\, mm^2$
$\delta = 0.43 \frac{\sum_{j=1}^{n} r_j \frac{\phi_j}{90}}{\sum_{i=1}^{m} b_{p,i}} = 0.031$ (EN 1993-1-3 (5.1))
$A_g = A_{g,sh}(1 - \delta) = 174(1 - 0.031) = 169\, mm^2$
$I_{g,x} = I_{g,sh,x}(1 - 2\delta) = 149352(1 - 2 \cdot 0.031) = 140121\, mm^4$
$I_{g,y} = I_{g,sh,y}(1 - 2\delta) = 37548(1 - 2 \cdot 0.031) = 35227\, mm^4$

2.3 Effective cross-section

$\chi_d = 0.944$ after 2 iterations

2.3.1 Upper lip

$k_\sigma = 0.430$ (EN 1993-1-5, Table 4.2)
$\bar{\lambda}_p = \chi_d \frac{b/t}{28.4\epsilon\sqrt{k_\sigma}} = 0.944 \frac{14/1.0}{28.4 \cdot 0.97 \cdot \sqrt{0.4}} = 0.738$
for outstanding element and $\bar{\lambda}_p \leq 0.748$ $\rho = 1$ (EN 1993-1-5 (4.3))

2.3.2 Web

$k_\sigma = 4.000$ (EN 1993-1-5, Table 4.1)
$\bar{\lambda}_p = \frac{b/t}{28.4\epsilon\sqrt{k_\sigma}} = \frac{70/1.0}{28.4 \cdot 0.97 \cdot \sqrt{4.0}} = 1.276$
for internal element and $\bar{\lambda}_p > 0.673$
$\rho = \frac{\bar{\lambda}_p - 0.055(3+\psi)}{\bar{\lambda}_p^2} = \frac{1.28 - 0.055(3+1.0)}{1.28^2} = 0.649$ (EN 1993-1-5 (4.2))

2.3.3 Lower lip

$k_\sigma = 0.430$ (EN 1993-1-5, Table 4.2)
$\bar{\lambda}_p = \chi_d \frac{b/t}{28.4\epsilon\sqrt{k_\sigma}} = 0.944 \frac{14/1.0}{28.4 \cdot 0.97 \cdot \sqrt{0.4}} = 0.738$
for outstanding element and $\bar{\lambda}_p \leq 0.748$ $\rho = 1$ (EN 1993-1-5 (4.3))

2.3.4 The effect of edge stiffeners

$\sigma_{com,Ed} = f_y = 250.000\, MPa$
$k_f = \frac{A_{s2}}{A_{s1}} = \frac{33.0}{33.0} = 1.000$
$K = \frac{Et^3}{4(1-\nu^2)} \cdot \frac{1}{b_1^2 h_w + b_1^3 + 0{,}5 b_1 b_2 h_w k_f} = \frac{200000 \cdot 1.0^3}{4(1-0.3^2)} \cdot \frac{1}{31^2 \cdot 72 + 31^3 + 0{,}5 \cdot 31 \cdot 31 \cdot 72 \cdot 1} = 0.41$
$\sigma_{cr,s} = \frac{2\sqrt{KEI_s}}{A_s} = \frac{2\sqrt{0.4 \cdot 200000 \cdot 743}}{33.0} = 472.3\, MPa$
$\bar{\lambda}_d = \sqrt{\frac{f_y}{\sigma_{cr,s}}} = \sqrt{\frac{250.0}{472.3}} = 0.728$
$\chi_d = 1{,}47 - 0{,}723\bar{\lambda}_d = 1{,}47 - 0{,}723 \cdot 0.7 = 0.944$ for $\bar{\lambda}_d \leq 1.38$
$A_{s,red} = \chi_d A_s = 0.944 \cdot 33.0 = 28.3\, mm^2$

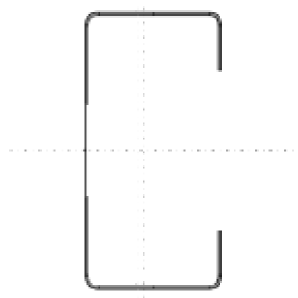

Figure 2: Effective section of Lipped channel 36.0x72.0x15.0 1.0 mm

2.3.5 Sectional properties

$A_{eff} = 141\, mm^2$
$I_{x,eff} = 144089\, mm^4$
$I_{y,eff} = 31183\, mm^4$
$e_x = 1.87\, mm$

2.4 Member buckling resistance

Buckling curve d, $\alpha = 0.76$, $\bar{\lambda}_0 = 0.2$ $i_0 = \sqrt{i_x^2 + i_y^2 + x_0^2} = \sqrt{32.0^2 + 14.9^2 + 33.6^2} = 48.7\, mm$

$N_{cr,x} = \frac{\pi^2 E I_x}{L_{cr,x}^2} = \frac{\pi^2 200000 \cdot 144089}{1000^2} = 284.4\ kN$
$N_{cr,y} = \frac{\pi^2 E I_y}{L_{cr,y}^2} = \frac{\pi^2 200000 \cdot 31183}{1000^2} = 61.6\ kN$
$N_{cr,T} = \frac{1}{i_0^2}(G I_t + \frac{\pi^2 E I_w}{L_{cr,T}^2}) = \frac{1}{48.734^2}(76923 \cdot 56 + \frac{\pi^2 200000 \cdot 61567855}{1000^2}) = 44.7\ kN$
$\beta = 1 - (\frac{x_0}{r_0})^2 = 0.525$
$N_{cr,TF} = \frac{1}{2\beta}[N_{cr,T} + N_{cr,x} - \sqrt{(N_{cr,T} + N_{cr,x})^2 - 4\beta N_{cr,T} N_{cr,x}}] = 41.3\ kN$
$N_{cr} = min(N_{cr,TF}, N_{cr,y}) = 41.3\ kN$ (singly symmetric section)
$\bar{\lambda} = \sqrt{\frac{A f_y}{N_{cr}}} = \sqrt{\frac{141 \cdot 250}{41338.2}} = 0.922$
$\phi = \frac{1}{2}(1 + \alpha(\bar{\lambda} - \bar{\lambda}_0) + \bar{\lambda}^2) = \frac{1}{2}(1 + 0.76(0.92 - 0.2) + 0.92^2) = 1.200$
$\chi = \frac{1}{\phi + \sqrt{\phi^2 - \bar{\lambda}^2}} = \frac{1}{1.20 + \sqrt{1.20^2 - 0.92^2}} \leq 1\ \chi = 0.508$
$N_{b,Rk} = \chi A f_y = 0.51 \cdot 141 \cdot 250 = 17.9\ kN$

3 Compression resistance according to EN 1993 rules for stainless steel modified by Talja and Salmi

3.1 Gross cross-section

$A_{real} = 169\,mm^2$
$A_{g,sh} = \sum_{i=1}^{m} b_i ti = 174\,mm^2$
$I_{g,sh,x} = 149352\,mm^2$
$I_{g,sh,y} = 37548\,mm^2$
$\delta = 0.43 \frac{\sum_{j=1}^{n} r_j \frac{\phi_j}{90}}{\sum_{i=1}^{m} b_{p,i}} = 0.031$ (EN 1993-1-3 (5.1))
$A_g = A_{g,sh}(1-\delta) = 174(1-0.031) = 169\,mm^2$
$I_{g,x} = I_{g,sh,x}(1-2\delta) = 149352(1-2\cdot 0.031) = 140121\,mm^4$
$I_{g,y} = I_{g,sh,y}(1-2\delta) = 37548(1-2\cdot 0.031) = 35227\,mm^4$

3.2 Member buckling resistance

$\alpha = 0.49,\ \bar{\lambda}_0 = 0.4$
$i_0 = \sqrt{i_x^2 + i_y^2 + x_0^2} = \sqrt{29.7^2 + 14.9^2 + 33.6^2} = 47.3\,mm$
$N_{cr,x} = \frac{\pi^2 E I_x}{L_{cr,x}^2} = \frac{\pi^2 200000 \cdot 149352}{1000^2} = 294.8\,kN$
$N_{cr,y} = \frac{\pi^2 E I_y}{L_{cr,y}^2} = \frac{\pi^2 200000 \cdot 37548}{1000^2} = 74.1\,kN$
$N_{cr,T} = \frac{1}{i_0^2}(G I_t + \frac{\pi^2 E I_w}{L_{cr,T}^2}) = \frac{1}{47.282^2}(76923 \cdot 56 + \frac{\pi^2 200000 \cdot 51567855}{1000^2}) = 47.5\,kN$
$\beta = 1 - (\frac{x_0}{r_0})^2 = 0.495$
$N_{cr,TF} = \frac{1}{2\beta}[N_{cr,T} + N_{cr,x} - \sqrt{(N_{cr,T} + N_{cr,x})^2 - 4\beta N_{cr,T} N_{cr,x}}] = 43.6\,kN$
$N_{cr} = min(N_{cr,TF}, N_{cr,y}) = 43.6\,kN$ (singly symmetric section)
$\bar{\lambda} = \sqrt{\frac{A f_y}{N_{cr}}} = \sqrt{\frac{169 \cdot 250}{43638.7}} = 0.984$
$\phi = \frac{1}{2}(1 + \alpha(\bar{\lambda} - \bar{\lambda}_0) + \bar{\lambda}^2) = \frac{1}{2}(1 + 0.49(0.98 - 0.4) + 0.98^2) = 1.127$
$\chi = \frac{1}{\phi + \sqrt{\phi^2 - \bar{\lambda}^2}} = \frac{1}{1.13 + \sqrt{1.13^2 - 0.98^2}} \leq 1\ \chi = 0.597$

3.3 Cross-section classification

Upper lip: $c/t = 15/1.0 = 15.0 > 11.3$ Class 4
Upper flange: $c/t = 36/1.0 = 36.0 > 29.0$ Class 4
Web: $c/t = 72/1.0 = 72.0 > 29.0$ Class 4
Lower flange: $c/t = 36/1.0 = 36.0 > 29.0$ Class 4
Lower lip: $c/t = 15/1.0 = 15.0 > 11.3$ Class 4
Class 4 cross-section.

3.4 Effective cross-section

$\chi_d = 0.945$ after 4 iterations

3.4.1 Upper lip

$k_\sigma = 0.430$ (EN 1993-1-5, Table 4.2)
$\bar{\lambda}_p = \chi_d \sqrt{\chi} \frac{b/t}{28.4\epsilon\sqrt{k_\sigma}} = 0.945\sqrt{0.597}\frac{14/1.0}{28.4 \cdot 0.97 \cdot \sqrt{0.4}} = 0.571$
for outstanding element $\rho = 1$ (EN 1993-1-4)

3.4.2 Upper flange

$k_\sigma = 4.000$ (EN 1993-1-5, Table 4.1)
$\bar{\lambda}_p = \chi_d \sqrt{\chi} \frac{b/t}{28.4\epsilon\sqrt{k_\sigma}} = 0.945\sqrt{0.597}\frac{34/1.0}{28.4 \cdot 0.97 \cdot \sqrt{4.0}} = 0.454$
for internal element $\rho = \frac{0.722}{\bar{\lambda}_p} - \frac{0.125}{\bar{\lambda}_p^2} = \frac{0.722}{0.45} - \frac{0.125}{0.45^2} = 0.984$ (EN 1993-1-4)

3.4.3 Web

$k_\sigma = 4.000$ (EN 1993-1-5, Table 4.1)
$\bar{\lambda}_p = \sqrt{\chi} \frac{b/t}{28.4\epsilon\sqrt{k_\sigma}} = \sqrt{0.597}\frac{70/1.0}{28.4 \cdot 0.97 \cdot \sqrt{4.0}} = 0.985$
for internal element $\rho = \frac{0.722}{\bar{\lambda}_p} - \frac{0.125}{\bar{\lambda}_p^2} = \frac{0.722}{0.99} - \frac{0.125}{0.99^2} = 0.604$ (EN 1993-1-4)

3.4.4 Lower flange

$k_\sigma = 4.000$ (EN 1993-1-5, Table 4.1)
$\bar{\lambda}_p = \chi_d \sqrt{\chi} \frac{b/t}{28.4\epsilon\sqrt{k_\sigma}} = 0.945\sqrt{0.597}\frac{34/1.0}{28.4 \cdot 0.97 \cdot \sqrt{4.0}} = 0.454$
for internal element $\rho = \frac{0.722}{\bar{\lambda}_p} - \frac{0.125}{\bar{\lambda}_p^2} = \frac{0.722}{0.45} - \frac{0.125}{0.45^2} = 0.984$ (EN 1993-1-4)

3.4.5 Lower lip

$k_\sigma = 0.430$ (EN 1993-1-5, Table 4.2)
$\bar{\lambda}_p = \chi_d \sqrt{\chi} \frac{b/t}{28.4\epsilon\sqrt{k_\sigma}} = 0.945\sqrt{0.597}\frac{14/1.0}{28.4 \cdot 0.97 \cdot \sqrt{0.4}} = 0.571$
for outstanding element $\rho = 1$ (EN 1993-1-4)

3.4.6 The effect of edge stiffeners

$\sigma_{com,Ed} = f_y = 250.000\,MPa$
$k_f = \frac{A_{s2}}{A_{s1}} = \frac{32.7}{32.7} = 1.000$
$K = \frac{Et^3}{4(1-\nu^2)} \cdot \frac{1}{b_1^2 h_w + b_1^3 + 0,5 b_1 b_2 h_w k_f} = \frac{200000 \cdot 1.0^3}{4(1-0.3^2)} \cdot \frac{1}{31^2 \cdot 72 + 31^3 + 0,5 \cdot 31 \cdot 31 \cdot 72 \cdot 1} = 0.41$
$\sigma_{cr,s} = \frac{2\sqrt{K E I_s}}{A_s} = \frac{2\sqrt{0.4 \cdot 200000 \cdot 740}}{32.7} = 473.4\,MPa$
$\bar{\lambda}_d = \sqrt{\frac{f_y}{\sigma_{cr,s}}} = \sqrt{\frac{250.0}{473.4}} = 0.727$
$\chi_d = 1,47 - 0,723\bar{\lambda}_d = 1,47 - 0,723 \cdot 0.7 = 0.945$ for $\bar{\lambda}_d \leq 1.38$
$A_{s,red1} = \chi_{d1} A_{s1} = 0.945 \cdot 32.7 = 28.1\,mm^2$

$A_{s,red2} = \chi_{d1} A_{s2} = 0.945 \cdot 32.7 = 28.1\,mm^2$

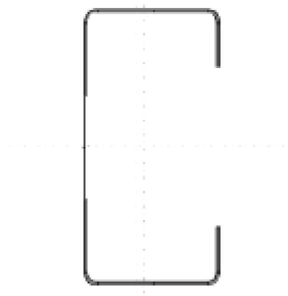

Figure 3: Effective section of Lipped channel 36.0x72.0x15.0 1.0 mm

3.4.7 Sectional properties

$A_{eff} = 136\,mm^2$
$I_{x,eff} = 142221\,mm^4$
$I_{y,eff} = 30414\,mm^4$
$e_x = 2.20\,mm$
$N_{b,Rk} = \chi A f_y = 0.60 \cdot 136 \cdot 250 = 20.4\,kN$

4 Compression resistance using DSM according to Becque et al. for EN 1993

$A_{real} = 169\,mm^2$
$A_{g,sh} = \sum_{i=1}^{m} b_i ti = 174\,mm^2$
$I_{g,sh,x} = 149352\,mm^2$
$I_{g,sh,y} = 37548\,mm^2$
$\delta = 0.43 \frac{\sum_{j=1}^{n} r_j \frac{\phi_j}{90}}{\sum_{i=1}^{m} b_{p,i}} = 0.031$ (EN 1993-1-3 (5.1))
$A_g = A_{g,sh}(1-\delta) = 174(1-0.031) = 169\,mm^2$
$I_{g,x} = I_{g,sh,x}(1-2\delta) = 149352(1-2\cdot 0.031) = 140121\,mm^4$
$I_{g,y} = I_{g,sh,y}(1-2\delta) = 37548(1-2\cdot 0.031) = 35227\,mm^4$

4.1 Distortional buckling

$k_f = \frac{A_{s2}}{A_{s1}} = \frac{51.0}{51.0} = 1.000$
$K = \frac{Et^3}{4(1-\nu^2)} \cdot \frac{1}{b_1^2 h_w + b_1^3 + 0{,}5 b_1 b_2 h_w k_f} = \frac{200000\cdot 1.0^3}{4(1-0.3^2)} \cdot \frac{1}{23^2\cdot 72 + 23^3 + 0{,}5\cdot 23\cdot 23\cdot 72\cdot 1} = 0.77$
$\sigma_{cr,s} = \frac{2\sqrt{K E I_s}}{A_s} = \frac{2\sqrt{0.8\cdot 200000\cdot 880}}{51.0} = 456.8\,MPa$
$\lambda = \sqrt{\frac{f_y}{\sigma_{cr}}} = \sqrt{\frac{250}{457}} = 0.740$
$f_{y,red} = (\frac{0.90}{0.74^{1.10}} - \frac{0.20}{0.74^{2.20}})f_y = 216\,MPa$ for $\lambda > 0.533$
$N_b = f_{y,red}A = 216\cdot 169 = 36.5\,kN$

4.2 Overall and local buckling interaction

$\sigma_{cr} = k\frac{\pi^2 E}{12(1-\nu)^2}(\frac{t}{b})^2 = 4.0\frac{\pi^2 200000}{12(1-0.3)^2}(\frac{1.0}{66})^2 = 308\,MPa$
(for Web) $\alpha = 0.49$, $\bar{\lambda}_0 = 0.4$
$i_0 = \sqrt{i_x^2 + i_y^2 + x_0^2} = \sqrt{29.7^2 + 14.9^2 + 33.6^2} = 47.3\,mm$
$N_{cr,x} = \frac{\pi^2 EI_x}{L_{cr,x}^2} = \frac{\pi^2 200000\cdot 149352}{1000^2} = 294.8\,kN$
$N_{cr,y} = \frac{\pi^2 EI_y}{L_{cr,y}^2} = \frac{\pi^2 200000\cdot 37548}{1000^2} = 74.1\,kN$
$N_{cr,T} = \frac{1}{i_0^2}(GI_t + \frac{\pi^2 EI_w}{L_{cr,T}^2}) = \frac{1}{47.282^2}(76923\cdot 56 + \frac{\pi^2 200000\cdot 51567855}{1000^2}) = 47.5\,kN$
$\beta = 1 - (\frac{x_0}{r_0})^2 = 0.495$
$N_{cr,TF} = \frac{1}{2\beta}[N_{cr,T} + N_{cr,x} - \sqrt{(N_{cr,T}+N_{cr,x})^2 - 4\beta N_{cr,T}N_{cr,x}}] = 43.6\,kN$
$N_{cr} = min(N_{cr,TF}, N_{cr,y}) = 43.6\,kN$ (singly symmetric section)
$\bar{\lambda} = \sqrt{\frac{Af_y}{N_{cr}}} = \sqrt{\frac{169\cdot 250}{43638.7}} = 0.984$
$\phi = \frac{1}{2}(1 + \alpha(\bar{\lambda} - \bar{\lambda}_0) + \bar{\lambda}^2) = \frac{1}{2}(1 + 0.49(0.98 - 0.4) + 0.98^2) = 1.127$
$\chi = \frac{1}{\phi + \sqrt{\phi^2 - \bar{\lambda}^2}} = \frac{1}{1.13 + \sqrt{1.13^2 - 0.98^2}} \leq 1\, \chi = 0.597$
$\lambda = \sqrt{\frac{\chi f_y}{\sigma_{cr}}} = \sqrt{\frac{0.597\cdot 250}{308}} = 0.696$
$f_{y,red} = (\frac{0.95}{0.70^{1.00}} - \frac{0.20}{0.70^{2.00}})f_y = 238\,MPa$ for $\lambda > 0.550$

$$N_b = \chi f_{y,red} A = 0.597 \cdot 238 \cdot 169 = 24.0\ kN$$

5 Compression resistance using CSM

$\sigma_{cr} = k\frac{\pi^2 E}{12(1-\nu)^2}(\frac{t}{b})^2 = 4.0\frac{\pi^2 200000}{12(1-0.3)^2}(\frac{1.0}{66})^2 = 308\,MPa$
$\lambda_p = \sqrt{\frac{f_y}{\sigma_{cr}}} = \sqrt{\frac{250}{308}} = 0.901$
$\lambda_{cs} = max(\lambda_p) = 0.901$ for Web
$\frac{\epsilon_{csm}}{\epsilon_y} = \frac{0.25}{\sigma_{cs}{}^{3.6}} = \frac{0.25}{0.901} = 0.365\ \leq (15, \frac{0.1\epsilon_u}{\epsilon_y} = \frac{0.1 \cdot 0.286}{0.001})$
$f_{csm} = f_y + E_{sh}\epsilon_y(\frac{\epsilon_{csm}}{\epsilon_y} - 1) = 250 + 2355 \cdot 0.001(0.365 - 1) = 248.129\,MPa$
$N_{csm,Rk} = f_{csm}A = 250 \cdot 169 = 41.897\,kN$

6 Effective sections reduction factors

EN 1993-1-4 width reduction

	0.5 mm	1.0 mm	1.5 mm
Web	0.264	0.489	0.676
Upper lip	0.734	0.935	1.000
Upper flange	0.678	0.871	1.000
Lower flange	0.678	0.871	1.000
Lower lip	0.734	0.935	1.000

EN 1993-1-4 thickness reduction

	0.5 mm	1.0 mm	1.5 mm
Upper lip	0.682	0.936	1.000
Upper flange	0.682	0.936	1.000
Lower flange	0.682	0.936	1.000
Lower lip	0.682	0.936	1.000

EN 1993-1-1 width reduction

	0.5 mm	1.0 mm	1.5 mm
Web	0.358	0.649	0.872
Upper lip	0.765	1.000	1.000
Upper flange	0.867	1.000	1.000
Lower flange	0.867	1.000	1.000
Lower lip	0.765	1.000	1.000

EN 1993-1-1 thickness reduction

	0.5 mm	1.0 mm	1.5 mm
Upper lip	0.690	0.944	1.000
Upper flange	0.690	0.944	1.000
Lower flange	0.690	0.944	1.000
Lower lip	0.690	0.944	1.000

Compressive strength of Section B (Lipped channel 24x72 mm)

Petr Hradil

March 28, 2013

Contents

1 Compression resistance according to EN 1993 rules for stainless steel

1.1 Cross-section classification

Upper lip: $c/t = 15/1.0 = 15.0 > 11.3$ Class 4
Upper flange: $c/t = 24/1.0 = 24.0 \leq 29.0$ Class 3
Web: $c/t = 72/1.0 = 72.0 > 29.0$ Class 4
Lower flange: $c/t = 24/1.0 = 24.0 \leq 29.0$ Class 3
Lower lip: $c/t = 15/1.0 = 15.0 > 11.3$ Class 4
Class 4 cross-section.

1.2 Gross cross-section

$A_{real} = 145\,mm^2$
$A_{g,sh} = \sum_{i=1}^{m} b_i ti = 150\,mm^2$
$I_{g,sh,x} = 118246\,mm^2$
$I_{g,sh,y} = 15307\,mm^2$
$\delta = 0.43 \frac{\sum_{j=1}^{n} r_j \frac{\phi_j}{90}}{\sum_{i=1}^{m} b_{p,i}} = 0.036$ (EN 1993-1-3 (5.1))
$A_g = A_{g,sh}(1-\delta) = 150(1-0.036) = 145\,mm^2$
$I_{g,x} = I_{g,sh,x}(1-2\delta) = 118246(1-2\cdot 0.036) = 109711\,mm^4$
$I_{g,y} = I_{g,sh,y}(1-2\delta) = 15307(1-2\cdot 0.036) = 14202\,mm^4$

1.3 Effective cross-section

$\chi_d = 1.000$ after 1 iterations

1.3.1 Upper lip

$k_\sigma = 0.430$ (EN 1993-1-5, Table 4.2)
$\bar{\lambda}_p = \frac{b/t}{28.4\epsilon\sqrt{k_\sigma}} = \frac{14/1.0}{28.4 \cdot 0.97 \cdot \sqrt{0.4}} = 0.782$
for outstanding element $\rho = \frac{1.0}{\bar{\lambda}_p} - \frac{0.231}{\bar{\lambda}_p^2} = \frac{1.0}{0.78} - \frac{0.231}{0.78^2} = 0.901$ (EN 1993-1-4)

1.3.2 Web

$k_\sigma = 4.000$ (EN 1993-1-5, Table 4.1)
$\bar{\lambda}_p = \frac{b/t}{28.4\epsilon\sqrt{k_\sigma}} = \frac{70/1.0}{28.4 \cdot 0.97 \cdot \sqrt{4.0}} = 1.276$
for internal element $\rho = \frac{0.722}{\bar{\lambda}_p} - \frac{0.125}{\bar{\lambda}_p^2} = \frac{0.722}{1.28} - \frac{0.125}{1.28^2} = 0.489$ (EN 1993-1-4)

1.3.3 Lower lip

$k_\sigma = 0.430$ (EN 1993-1-5, Table 4.2)

$\bar{\lambda}_p = \frac{b/t}{28.4\epsilon\sqrt{k_\sigma}} = \frac{14/1.0}{28.4 \cdot 0.97 \cdot \sqrt{0.4}} = 0.782$

for outstanding element $\rho = \frac{1.0}{\bar{\lambda}_p} - \frac{0.231}{\bar{\lambda}_p^2} = \frac{1.0}{0.78} - \frac{0.231}{0.78^2} = 0.901$ (EN 1993-1-4)

1.3.4 The effect of edge stiffeners

$\sigma_{com,Ed} = f_y = 250.000\,MPa$

$k_f = \frac{A_{s2}}{A_{s1}} = \frac{25.6}{25.6} = 1.000$

$K = \frac{Et^3}{4(1-\nu^2)} \cdot \frac{1}{b_1^2 h_w + b_1^3 + 0{,}5 b_1 b_2 h_w k_f} = \frac{200000 \cdot 1.0^3}{4(1-0.3^2)} \cdot \frac{1}{21^2 \cdot 72 + 21^3 + 0{,}5 \cdot 21 \cdot 21 \cdot 72 \cdot 1} = 0.95$

$\sigma_{cr,s} = \frac{2\sqrt{KEI_s}}{A_s} = \frac{2\sqrt{0.9 \cdot 200000 \cdot 506}}{25.6} = 764.6\,MPa$

$\bar{\lambda}_d = \sqrt{\frac{f_y}{\sigma_{cr,s}}} = \sqrt{\frac{250.0}{764.6}} = 0.572$

$\chi_d = 1.0$ for $\bar{\lambda}_d \leq 0.65$

$A_{s,red} = \chi_d A_s = 1.000 \cdot 25.6 = 23.3\,mm^2$

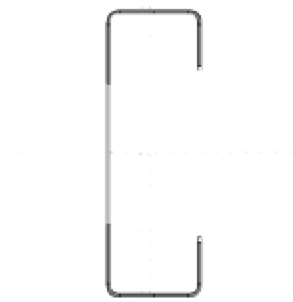

Figure 1: Effective section of Lipped channel 24.0x72.0x15.0 1.0 mm

1.3.5 Sectional properties

$A_{eff} = 106\,mm^2$

$I_{x,eff} = 113080\,mm^4$

$I_{y,eff} = 11325\,mm^4$

$e_x = 2.40\,mm$

1.4 Member buckling resistance

$\alpha = 0.49$, $\bar{\lambda}_0 = 0.4$

$i_0 = \sqrt{i_x^2 + i_y^2 + x_0^2} = \sqrt{32.6^2 + 10.3^2 + 22.3^2} = 40.8\,mm$

$N_{cr,x} = \frac{\pi^2 EI_x}{L_{cr,x}^2} = \frac{\pi^2 200000 \cdot 113080}{1000^2} = 223.2\,kN$

$N_{cr,y} = \frac{\pi^2 EI_y}{L_{cr,y}^2} = \frac{\pi^2 200000 \cdot 11326}{1000^2} = 22.4\,kN$

$N_{cr,T} = \frac{1}{i_0^2}(GI_t + \frac{\pi^2 EI_w}{L_{cr,T}^2}) = \frac{1}{40.836^2}(76923 \cdot 48 + \frac{\pi^2 200000 \cdot 21204042}{1000^2}) = 27.3\,kN$

$\beta = 1 - (\frac{x_0}{r_0})^2 = 0.703$

$N_{cr,TF} = \frac{1}{2\beta}[N_{cr,T} + N_{cr,x} - \sqrt{(N_{cr,T} + N_{cr,x})^2 - 4\beta N_{cr,T} N_{cr,x}}] = 26.3\,kN$

$N_{cr} = min(N_{cr,TF}, N_{cr,y}) = 22.4\,kN$ (singly symmetric section)

$\bar{\lambda} = \sqrt{\frac{Af_y}{N_{cr}}} = \sqrt{\frac{106 \cdot 250}{22354.7}} = 1.090$

$\phi = \frac{1}{2}(1 + \alpha(\bar{\lambda} - \bar{\lambda}_0) + \bar{\lambda}^2) = \frac{1}{2}(1 + 0.49(1.09 - 0.4) + 1.09^2) = 1.263$

$\chi = \frac{1}{\phi + \sqrt{\phi^2 - \bar{\lambda}^2}} = \frac{1}{1.26 + \sqrt{1.26^2 - 1.09^2}} \leq 1\; \chi = 0.526$

$N_{b,Rk} = \chi A f_y = 0.53 \cdot 106 \cdot 250 = 14.0\,kN$

2 Compression resistance according to EN 1993 rules for carbon steel

2.1 Cross-section classification

Upper lip: $c/t = 15/1.0 = 15.0 > 13.6$ Class 4
Upper flange: $c/t = 24/1.0 = 24.0 \leq 40.7$ Class 3
Web: $c/t = 72/1.0 = 72.0 > 40.7$ Class 4
Lower flange: $c/t = 24/1.0 = 24.0 \leq 40.7$ Class 3
Lower lip: $c/t = 15/1.0 = 15.0 > 13.6$ Class 4
Class 4 cross-section.

2.2 Gross cross-section

$A_{real} = 145\, mm^2$
$A_{g,sh} = \sum_{i=1}^{m} b_i ti = 150\, mm^2$
$I_{g,sh,z} = 118246\, mm^2$
$I_{g,sh,y} = 15307\, mm^2$
$\delta = 0.43 \frac{\sum_{j=1}^{n} r_j \frac{\phi_j}{90}}{\sum_{i=1}^{m} b_{p,i}} = 0.036$ (EN 1993-1-3 (5.1))
$A_g = A_{g,sh}(1-\delta) = 150(1-0.036) = 145\, mm^2$
$I_{g,z} = I_{g,sh,z}(1-2\delta) = 118246(1-2\cdot 0.036) = 109711\, mm^4$
$I_{g,y} = I_{g,sh,y}(1-2\delta) = 15307(1-2\cdot 0.036) = 14202\, mm^4$

2.3 Effective cross-section

$\chi_d = 1.000$ after 1 iterations

2.3.1 Upper lip

$k_\sigma = 0.430$ (EN 1993-1-5, Table 4.2)
$\bar{\lambda}_p = \frac{b/t}{28.4\epsilon\sqrt{k_\sigma}} = \frac{14/1.0}{28.4 \cdot 0.97 \cdot \sqrt{0.4}} = 0.782$
for outstanding element and $\bar{\lambda}_p > 0.748$
$\rho = \frac{\bar{\lambda}_p - 0.188}{\bar{\lambda}_p^2} = \frac{0.78-0.188}{0.78^2} = 0.971$ (EN 1993-1-5 (4.3))

2.3.2 Web

$k_\sigma = 4.000$ (EN 1993-1-5, Table 4.1)
$\bar{\lambda}_p = \frac{b/t}{28.4\epsilon\sqrt{k_\sigma}} = \frac{70/1.0}{28.4 \cdot 0.97 \cdot \sqrt{4.0}} = 1.276$
for internal element and $\bar{\lambda}_p > 0.673$
$\rho = \frac{\bar{\lambda}_p - 0.055(3+\psi)}{\bar{\lambda}_p^2} = \frac{1.28-0.055(3+1.0)}{1.28^2} = 0.649$ (EN 1993-1-5 (4.2))

2.3.3 Lower lip

$k_\sigma = 0.430$ (EN 1993-1-5, Table 4.2)
$\bar{\lambda}_p = \frac{b/t}{28.4\epsilon\sqrt{k_\sigma}} = \frac{14/1.0}{28.4 \cdot 0.97 \cdot \sqrt{0.4}} = 0.782$
for outstanding element and $\bar{\lambda}_p > 0.748$
$\rho = \frac{\bar{\lambda}_p - 0.188}{\bar{\lambda}_p^2} = \frac{0.78 - 0.188}{0.78^2} = 0.971$ (EN 1993-1-5 (4.3))

2.3.4 The effect of edge stiffeners

$\sigma_{com,Ed} = f_y = 250.000\,MPa$
$k_f = \frac{A_{s2}}{A_{s1}} = \frac{26.6}{26.6} = 1.000$
$K = \frac{Et^3}{4(1-\nu^2)} \cdot \frac{1}{b_1^2 h_w + b_1^3 + 0{,}5 b_1 b_2 h_w k_f} = \frac{200000 \cdot 1.0^3}{4(1-0.3^2)} \cdot \frac{1}{21^2 \cdot 72 + 21^3 + 0{,}5 \cdot 21 \cdot 21 \cdot 72 \cdot 1} = 0.94$
$\sigma_{cr,s} = \frac{2\sqrt{KEI_s}}{A_s} = \frac{2\sqrt{0.9 \cdot 200000 \cdot 611}}{26.6} = 804.7\,MPa$
$\bar{\lambda}_d = \sqrt{\frac{f_y}{\sigma_{cr,s}}} = \sqrt{\frac{250.0}{804.7}} = 0.557$
$\chi_d = 1.0$ for $\bar{\lambda}_d \leq 0.65$
$A_{s,red} = \chi_d A_s = 1.000 \cdot 26.6 = 24.2\,mm^2$

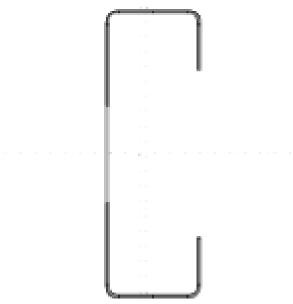

Figure 2: Effective section of Lipped channel 24.0x72.0x15.0 1.0 mm

2.3.5 Sectional properties

$A_{eff} = 119\,mm^2$
$I_{x,eff} = 116630\,mm^4$
$I_{y,eff} = 12948\,mm^4$
$e_x = 1.61\,mm$

2.4 Member buckling resistance

Buckling curve d, $\alpha = 0.76$, $\bar{\lambda}_0 = 0.2$ $i_0 = \sqrt{i_x^2 + i_y^2 + x_0^2} = \sqrt{31.3^2 + 10.4^2 + 22.3^2} = 39.8\,mm$

$N_{cr,x} = \frac{\pi^2 E I_x}{L_{cr,x}^2} = \frac{\pi^2 200000 \cdot 116630}{1000^2} = 230.2\,kN$

$N_{cr,y} = \frac{\pi^2 E I_y}{L_{cr,y}^2} = \frac{\pi^2 200000 \cdot 12948}{1000^2} = 25.6\,kN$

$N_{cr,T} = \frac{1}{i_0^2}(G I_t + \frac{\pi^2 E I_w}{L_{cr,T}^2}) = \frac{1}{39.767^2}(76923 \cdot 48 + \frac{\pi^2 200000 \cdot 21204042}{1000^2}) = 28.8\,kN$

$\beta = 1 - (\frac{x_0}{r_0})^2 = 0.686$

$N_{cr,TF} = \frac{1}{2\beta}[N_{cr,T} + N_{cr,x} - \sqrt{(N_{cr,T} + N_{cr,x})^2 - 4\beta N_{cr,T} N_{cr,x}}] = 27.6\,kN$

$N_{cr} = min(N_{cr,TF}, N_{cr,y}) = 25.6\,kN$ (singly symmetric section)

$\bar{\lambda} = \sqrt{\frac{A f_y}{N_{cr}}} = \sqrt{\frac{119 \cdot 250}{25558.9}} = 1.081$

$\phi = \frac{1}{2}(1 + \alpha(\bar{\lambda} - \bar{\lambda}_0) + \bar{\lambda}^2) = \frac{1}{2}(1 + 0.76(1.08 - 0.2) + 1.08^2) = 1.418$

$\chi = \frac{1}{\phi + \sqrt{\phi^2 - \bar{\lambda}^2}} = \frac{1}{1.42 + \sqrt{1.42^2 - 1.08^2}} \leq 1$ $\chi = 0.428$

$N_{b,Rk} = \chi A f_y = 0.43 \cdot 119 \cdot 250 = 12.8\,kN$

3 Compression resistance according to EN 1993 rules for stainless steel modified by Talja and Salmi

3.1 Gross cross-section

$A_{real} = 145\,mm^2$
$A_{g,sh} = \sum_{i=1}^{m} b_i ti = 150\,mm^2$
$I_{g,sh,x} = 118246\,mm^2$
$I_{g,sh,y} = 15307\,mm^2$
$\delta = 0.43 \frac{\sum_{j=1}^{n} r_j \frac{\phi_j}{90}}{\sum_{i=1}^{m} b_{p,i}} = 0.036$ (EN 1993-1-3 (5.1))
$A_g = A_{g,sh}(1-\delta) = 150(1-0.036) = 145\,mm^2$
$I_{g,x} = I_{g,sh,x}(1-2\delta) = 118246(1-2 \cdot 0.036) = 109711\,mm^4$
$I_{g,y} = I_{g,sh,y}(1-2\delta) = 15307(1-2 \cdot 0.036) = 14202\,mm^4$

3.2 Member buckling resistance

$\alpha = 0.49$, $\bar{\lambda}_0 = 0.4$
$i_0 = \sqrt{i_x^2 + i_y^2 + x_0^2} = \sqrt{28.6^2 + 10.3^2 + 22.3^2} = 37.7\,mm$
$N_{cr,x} = \frac{\pi^2 EI_x}{L_{cr,x}^2} = \frac{\pi^2 200000 \cdot 118246}{1000^2} = 233.4\,kN$
$N_{cr,y} = \frac{\pi^2 EI_y}{L_{cr,y}^2} = \frac{\pi^2 200000 \cdot 15307}{1000^2} = 30.2\,kN$
$N_{cr,T} = \frac{1}{i_0^2}(GI_t + \frac{\pi^2 EI_w}{L_{cr,T}^2}) = \frac{1}{37.655^2}(76923 \cdot 48 + \frac{\pi^2 200000 \cdot 21204042}{1000^2}) = 32.1\,kN$
$\beta = 1 - (\frac{x_0}{r_0})^2 = 0.650$
$N_{cr,TF} = \frac{1}{2\beta}[N_{cr,T} + N_{cr,x} - \sqrt{(N_{cr,T} + N_{cr,x})^2 - 4\beta N_{cr,T} N_{cr,x}}] = 30.5\,kN$
$N_{cr} = min(N_{cr,TF}, N_{cr,y}) = 30.2\,kN$ (singly symmetric section)
$\bar{\lambda} = \sqrt{\frac{Af_y}{N_{cr}}} = \sqrt{\frac{145 \cdot 250}{30214.9}} = 1.095$
$\phi = \frac{1}{2}(1 + \alpha(\bar{\lambda} - \bar{\lambda}_0) + \bar{\lambda}^2) = \frac{1}{2}(1 + 0.49(1.09 - 0.4) + 1.09^2) = 1.269$
$\chi = \frac{1}{\phi + \sqrt{\phi^2 - \bar{\lambda}^2}} = \frac{1}{1.27 + \sqrt{1.27^2 - 1.09^2}} \leq 1\ \chi = 0.523$

3.3 Cross-section classification

Upper lip: $c/t = 15/1.0 = 15.0 > 11.3$ Class 4
Upper flange: $c/t = 24/1.0 = 24.0 \leq 29.0$ Class 3
Web: $c/t = 72/1.0 = 72.0 > 29.0$ Class 4
Lower flange: $c/t = 24/1.0 = 24.0 \leq 29.0$ Class 3
Lower lip: $c/t = 15/1.0 = 15.0 > 11.3$ Class 4
Class 4 cross-section.

3.4 Effective cross-section

$\chi_d = 1.000$ after 1 iterations

3.4.1 Upper lip

$k_\sigma = 0.430$ (EN 1993-1-5, Table 4.2)
$\bar{\lambda}_p = \sqrt{\chi}\frac{b/t}{28.4\epsilon\sqrt{k_\sigma}} = \sqrt{0.523}\frac{14/1.0}{28.4 \cdot 0.97 \cdot \sqrt{0.4}} = 0.566$
for outstanding element $\rho = 1$ (EN 1993-1-4)

3.4.2 Web

$k_\sigma = 4.000$ (EN 1993-1-5, Table 4.1)
$\bar{\lambda}_p = \sqrt{\chi}\frac{b/t}{28.4\epsilon\sqrt{k_\sigma}} = \sqrt{0.523}\frac{70/1.0}{28.4 \cdot 0.97 \cdot \sqrt{4.0}} = 0.922$
for internal element $\rho = \frac{0.722}{\bar{\lambda}_p} - \frac{0.125}{\bar{\lambda}_p^2} = \frac{0.722}{0.92} - \frac{0.125}{0.92^2} = 0.636$ (EN 1993-1-4)

3.4.3 Lower lip

$k_\sigma = 0.430$ (EN 1993-1-5, Table 4.2)
$\bar{\lambda}_p = \sqrt{\chi}\frac{b/t}{28.4\epsilon\sqrt{k_\sigma}} = \sqrt{0.523}\frac{14/1.0}{28.4 \cdot 0.97 \cdot \sqrt{0.4}} = 0.566$
for outstanding element $\rho = 1$ (EN 1993-1-4)

3.4.4 The effect of edge stiffeners

$\sigma_{com,Ed} = f_y = 250.000\,MPa$
$k_f = \frac{A_{s2}}{A_{s1}} = \frac{27.0}{27.0} = 1.000$
$K = \frac{Et^3}{4(1-\nu^2)} \cdot \frac{1}{b_1^2 h_w + b_1^3 + 0{,}5 b_1 b_2 h_w k_f} = \frac{200000 \cdot 1.0^3}{4(1-0.3^2)} \cdot \frac{1}{21^2 \cdot 72 + 21^3 + 0{,}5 \cdot 21 \cdot 21 \cdot 72 \cdot 1} = 0.93$
$\sigma_{cr,s} = \frac{2\sqrt{KEI_s}}{A_s} = \frac{2\sqrt{0.9 \cdot 200000 \cdot 657}}{27.0} = 820.5\,MPa$
$\bar{\lambda}_d = \sqrt{\frac{f_y}{\sigma_{cr,s}}} = \sqrt{\frac{250.0}{820.5}} = 0.552$
$\chi_d = 1.0$ for $\bar{\lambda}_d \leq 0.65$
$A_{s,red} = \chi_d A_s = 1.000 \cdot 27.0 = 24.5\,mm^2$

3.4.5 Sectional properties

$A_{eff} = 119\,mm^2$
$I_{x,eff} = 116851\,mm^4$
$I_{y,eff} = 13003\,mm^4$
$e_x = 1.78\,mm$
$N_{b,Rk} = \chi A f_y = 0.52 \cdot 119 \cdot 250 = 15.6\,kN$

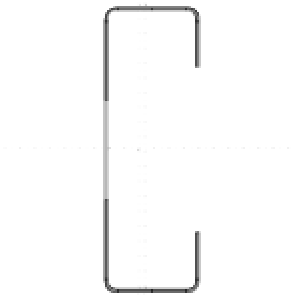

Figure 3: Effective section of Lipped channel 24.0x72.0x15.0 1.0 mm

4 Compression resistance using DSM according to Becque et al. for EN 1993

$A_{real} = 145\,mm^2$
$A_{g,sh} = \sum_{i=1}^{m} b_i ti = 150\,mm^2$
$I_{g,sh,x} = 118246\,mm^2$
$I_{g,sh,y} = 15307\,mm^2$
$\delta = 0.43 \frac{\sum_{j=1}^{n} r_j \frac{\phi_j}{90}}{\sum_{i=1}^{m} b_{p,i}} = 0.036$ (EN 1993-1-3 (5.1))
$A_g = A_{g,sh}(1-\delta) = 150(1-0.036) = 145\,mm^2$
$I_{g,x} = I_{g,sh,x}(1-2\delta) = 118246(1-2\cdot 0.036) = 109711\,mm^4$
$I_{g,y} = I_{g,sh,y}(1-2\delta) = 15307(1-2\cdot 0.036) = 14202\,mm^4$

4.1 Distortional buckling

$k_f = \frac{A_{s2}}{A_{s1}} = \frac{39.0}{39.0} = 1.000$
$K = \frac{Et^3}{4(1-\nu^2)} \cdot \frac{1}{b_1^2 h_w + b_1^3 + 0{,}5 b_1 b_2 h_w k_f} = \frac{200000\cdot 1.0^3}{4(1-0.3^2)} \cdot \frac{1}{17^2\cdot 72 + 17^3 + 0{,}5\cdot 17\cdot 17\cdot 72\cdot 1} = 1.60$
$\sigma_{cr,s} = \frac{2\sqrt{K\,EI_s}}{A_s} = \frac{2\sqrt{1.6\cdot 200000\cdot 802}}{39.0} = 821.0\,MPa$
$\lambda = \sqrt{\frac{f_y}{\sigma_{cr}}} = \sqrt{\frac{250}{821}} = 0.552$
$f_{y,red} = (\frac{0.90}{0.55^{1.10}} - \frac{0.20}{0.55^{2.20}})f_y = 248\,MPa$ for $\lambda > 0.533$
$N_b = f_{y,red} A = 248 \cdot 145 = 35.9\,kN$

4.2 Overall and local buckling interaction

$\sigma_{cr} = k\frac{\pi^2 E}{12(1-\nu)^2}(\frac{t}{b})^2 = 4.0\frac{\pi^2 200000}{12(1-0.3)^2}(\frac{1.0}{66})^2 = 308\,MPa$
(for Web) $\alpha = 0.49$, $\bar{\lambda}_0 = 0.4$
$i_0 = \sqrt{i_x^2 + i_y^2 + x_0^2} = \sqrt{28.6^2 + 10.3^2 + 22.3^2} = 37.7\,mm$
$N_{cr,x} = \frac{\pi^2 EI_x}{L_{cr,x}^2} = \frac{\pi^2 200000 \cdot 118246}{1000^2} = 233.4\,kN$
$N_{cr,y} = \frac{\pi^2 EI_y}{L_{cr,y}^2} = \frac{\pi^2 200000 \cdot 15307}{1000^2} = 30.2\,kN$
$N_{cr,T} = \frac{1}{i_0^2}(GI_t + \frac{\pi^2 EI_w}{L_{cr,T}^2}) = \frac{1}{37.655^2}(76923 \cdot 48 + \frac{\pi^2 200000 \cdot 21204042}{1000^2}) = 32.1\,kN$
$\beta = 1 - (\frac{x_0}{r_0})^2 = 0.650$
$N_{cr,TF} = \frac{1}{2\beta}[N_{cr,T} + N_{cr,x} - \sqrt{(N_{cr,T} + N_{cr,x})^2 - 4\beta N_{cr,T} N_{cr,x}}] = 30.5\,kN$
$N_{cr} = min(N_{cr,TF}, N_{cr,y}) = 30.2\,kN$ (singly symmetric section)
$\bar{\lambda} = \sqrt{\frac{Af_y}{N_{cr}}} = \sqrt{\frac{145 \cdot 250}{30214.9}} = 1.095$
$\phi = \frac{1}{2}(1 + \alpha(\bar{\lambda} - \bar{\lambda}_0) + \bar{\lambda}^2) = \frac{1}{2}(1 + 0.49(1.09 - 0.4) + 1.09^2) = 1.269$
$\chi = \frac{1}{\phi + \sqrt{\phi^2 - \bar{\lambda}^2}} = \frac{1}{1.27 + \sqrt{1.27^2 - 1.09^2}} \leq 1\ \chi = 0.523$
$\lambda = \sqrt{\frac{\chi f_y}{\sigma_{cr}}} = \sqrt{\frac{0.523 \cdot 250}{308}} = 0.651$
$f_{y,red} = (\frac{0.95}{0.65^{1.00}} - \frac{0.20}{0.65^{2.00}})f_y = 247\,MPa$ for $\lambda > 0.550$
$N_b = \chi f_{y,red} A = 0.523 \cdot 247 \cdot 145 = 18.7\,kN$

5 Compression resistance using CSM

$\sigma_{cr} = k\frac{\pi^2 E}{12(1-\nu)^2}(\frac{t}{b})^2 = 4.0\frac{\pi^2 200000}{12(1-0.3)^2}(\frac{1.0}{66})^2 = 308\; MPa$

$\lambda_p = \sqrt{\frac{f_y}{\sigma_{cr}}} = \sqrt{\frac{250}{308}} = 0.901$

$\lambda_{cs} = max(\lambda_p) = 0.901$ for Web

$\frac{\epsilon_{csm}}{\epsilon_y} = \frac{0.25}{\sigma_{cs}{}^{3.6}} = \frac{0.25}{0.901} = 0.365 \leq (15, \frac{0.1\epsilon_u}{\epsilon_y} = \frac{0.1 \cdot 0.286}{0.001})$

$f_{csm} = f_y + E_{sh}\epsilon_y(\frac{\epsilon_{csm}}{\epsilon_y} - 1) = 250 + 2355 \cdot 0.001(0.365 - 1) = 248.129\; MPa$

$N_{csm,Rk} = f_{csm}A = 250 \cdot 145 = 35.941\; kN$

6 Effective sections reduction factors

EN 1993-1-4 width reduction

	0.5 mm	1.0 mm	1.5 mm
Web	0.264	0.489	0.676
Upper lip	0.636	0.901	1.000
Upper flange	0.802	1.000	1.000
Lower flange	0.802	1.000	1.000
Lower lip	0.636	0.901	1.000

EN 1993-1-4 thickness reduction

	0.5 mm	1.0 mm	1.5 mm
Upper lip	0.825	1.000	1.000
Upper flange	0.825	1.000	1.000
Lower flange	0.825	1.000	1.000
Lower lip	0.825	1.000	1.000

EN 1993-1-1 width reduction

	0.5 mm	1.0 mm	1.5 mm
Web	0.358	0.649	0.872
Upper lip	0.660	0.971	1.000
Lower lip	0.660	0.971	1.000

EN 1993-1-1 thickness reduction

	0.5 mm	1.0 mm	1.5 mm
Upper lip	0.828	1.000	1.000
Upper flange	0.828	1.000	1.000
Lower flange	0.828	1.000	1.000
Lower lip	0.828	1.000	1.000